

This paper is published as part of a *Dalton Transactions* themed issue on:

Metal Anticancer Compounds

Guest Editor Peter Sadler

University of Warwick, UK

Published in [issue 48, 2009](#) of *Dalton Transactions*



Image reproduced with permission of Chi-Ming Che

Articles published in this issue include:

PERSPECTIVES:

[Non-traditional platinum compounds for improved accumulation, oral bioavailability, and tumor targeting](#)

Katherine S. Lovejoy and Stephen J. Lippard, *Dalton Trans.*, 2009, DOI: 10.1039/b913896j

[Metal complexes as photochemical nitric oxide precursors: Potential applications in the treatment of tumors](#)

Alexis D. Ostrowski and Peter C. Ford, *Dalton Trans.*, 2009, DOI: 10.1039/b912898k

[Novel and emerging approaches for the delivery of metallo-drugs](#)

Carlos Sanchez-Cano and Michael J. Hannon, *Dalton Trans.*, 2009, DOI: 10.1039/b912708a

HOT ARTICLE:

[Iron\(III\) complexes of fluorescent hydroxamate ligands: preparation, properties, and cellular processing](#)

Antonia J. Clarke, Natsuho Yamamoto, Paul Jensen and Trevor W. Hambley, *Dalton Trans.*, 2009, DOI: 10.1039/b914368h

Visit the *Dalton Transactions* website for more cutting-edge inorganic and bioinorganic research
www.rsc.org/dalton

Synthetic strategies towards ruthenium–porphyrin conjugates for anticancer activity†

Teresa Gianferrara,^{*a} Ioannis Bratsos,^b Elisabetta Iengo,^b Barbara Milani,^b Adrian Oštrić,^b Cinzia Spagnol,^a Ennio Zangrando^b and Enzo Alessio^{*b}

Received 11th June 2009, Accepted 31st July 2009

First published as an Advance Article on the web 27th August 2009

DOI: 10.1039/b911393b

The conjugation of porphyrins to metal fragments is a strategy for making new compounds that are expected to combine the phototoxicity and the tumour-localization properties of the porphyrin chromophore with the cytotoxicity of the metal fragment for additive antitumour effect. We report here the preparation of new classes of porphyrin–ruthenium conjugates with potential bio-medical applications. Ruthenium was chosen because several Ru compounds have shown promising anticancer activity. The conjugation with the porphyrin moiety was accomplished either through peripheral pyridyl rings (e.g. *meso*-4'-tetrapyrrolylporphyrin, 4'TPyP) or through bpy units (e.g. *meso*-(*p*-bpy-phenyl)porphyrins, bpy_{*n*}-PPs, *n* = 1–4). The number of Ru fragments attached to the porphyrins ranges from 1 to 4 and the total charge of the conjugates from –4 to +8. Different types of peripheral fragments, both Ru(III) and Ru(II), have been used: in some cases they are structurally similar to established anticancer compounds. Examples are [Na]₄[4'TPyP{*trans*-RuCl₂(dms_o-S)}₄] (**2**), that bears four NAMI-type Ru(III) fragments, or [4'TPyP{Ru([9]aneS3)(en)}₄][CF₃SO₃]₈ (**3**) and [bpy₄-PP{Ru([9]aneS3)(dms_o-S)}₄][CF₃SO₃]₈ (**9**) (en = ethane-1,2-diamine, [9]aneS3 = 1,4,7-trithiacyclononane) that have four half-sandwich Ru(II) compounds. The Ru fragments may either contain one or more labile ligands, such as in **2** or in **9**, or be coordinatively saturated and substitutionally inert, such as in **3** or in [bpy₄-PP{Ru([12]aneS4)}₄][CF₃SO₃]₈ (**11**) ([12]aneS4 = 1,4,7,10-tetrathiacyclododecane). Most of the ruthenium–porphyrin conjugates described in this work are soluble—at least moderately—in aqueous solution and are thus suitable for biological investigations, in particular for cytotoxicity and photo-cytotoxicity tests.

Introduction

Natural and synthetic porphyrins and metalloporphyrins are extensively investigated—and in some cases clinically applied—as photosensitizers in the photodynamic therapy of cancer (PDT).¹ PDT is a selective non-invasive therapy used in the early diagnosis and treatment of various neoplasms that combines the preferential uptake of photosensitizers into malignant tissues and their local irradiation with visible light.² Basically, two types of processes can occur in PDT after visible-light activation of the photosensitizer to its first excited triplet state (T₁), provided that T₁ is sufficiently long-lived. Type I PDT implies that the excited photosensitizer directly generates free radicals (mainly reactive oxygen species,

ROS) through electron—or hydrogen—transfer reactions, whereas the more common type II PDT is mediated by tissue oxygen: the excited photosensitizer converts normal triplet oxygen (³O₂) into singlet oxygen (¹O₂). The highly cytotoxic free radicals and/or singlet oxygen, through uncontrolled reactivity, induce cell death.³ Beside photoinduced cytotoxicity, some water-soluble porphyrins possess light-independent antiviral activity,⁴ whereas others have shown activity in the photoinactivation of pathogenic bacteria.⁵

Synthetic water-soluble porphyrins are typically obtained by functionalization of the chromophore, mainly at the *meso* positions, with hydrophilic or easily ionized groups. The conjugation of porphyrins to peripheral metal fragments is an intriguing alternative strategy for making water-soluble compounds. Such conjugates might have improved characteristics for biomedical applications (not limited to PDT): (i) they might combine the phototoxicity of the porphyrin chromophore to the cytotoxicity of the metal fragment for additive antitumour effect. (ii) They might have increased tumour selectivity. Porphyrins typically show preferential uptake and retention by tumour tissues (tumour-localization properties), possibly *via* receptor mediated endocytosis of low density lipoproteins (LDL) (cancer cells over-express LDL receptors).⁶ Thus, they might behave as carrier ligands for the active transport of anticancer metal fragments into cancer cells. (iii) Provided that the conjugates are sufficiently stable, the fluorescence emission of the chromophore might be exploited for tracking the biodistribution of the metal in the extra- and

^aDepartment of Pharmaceutical Sciences, University of Trieste, 34127, Trieste, Italy

^bDepartment of Chemical Sciences, University of Trieste, 34127, Trieste, Italy. E-mail: alessi@units.it

† Electronic supplementary information (ESI) available: Spectral data for selected *meso*-(*p*-nitrophenyl)porphyrins *p*(NO₂)_{*n*}PP (*n* = 1–4) and *meso*-(*p*-aminophenyl)porphyrins *p*(NH₂)_{*n*}PP (*n* = 1–4); time-evolution of the electronic absorption spectrum of **2**; ¹H NMR spectra of **3** and **12**; temperature dependence of the ¹H NMR spectra of **3** and **4**; details (BH resonances) of the ¹H NMR spectra of Bpy₂-*cis*PP and Bpy₂-*trans*PP; time-evolution of the ¹H NMR spectrum of **10**; schematic drawing of **4**; scheme of the preparation of **6**; fluorescence spectra of Bpy₄-PP and **9**; selected coordination bond lengths (Å) and angles (°) for **10**. CCDC reference numbers 735952 and 735953. For ESI and crystallographic data in CIF or other electronic format see DOI: 10.1039/b911393b

intra-cellular environment of malignant cells through fluorescence microscopy.

Not surprisingly, the first porphyrin-metal conjugates developed for biomedical applications concerned Pt(II) fragments structurally similar to the classical anticancer drugs cisplatin and carboplatin. Such compounds are expected to behave at the same time as photodynamic and chemotherapeutic agents.⁷⁻⁹ In addition, the high binding affinity of Pt(II) for nucleobases might help to localize the porphyrin close to DNA, thus enhancing the photo-induced damage.

Since several years also ruthenium compounds have attracted intense research interest as potential anticancer agents.¹⁰ Two Ru(III) coordination compounds, NAMI-A and KP1019 (Fig. 1), developed by us and by the group of Keppler, respectively,^{11,12} have completed phase 1 clinical trials and have started already (NAMI-A), or are scheduled to start soon (KP1019), a phase 2 study.

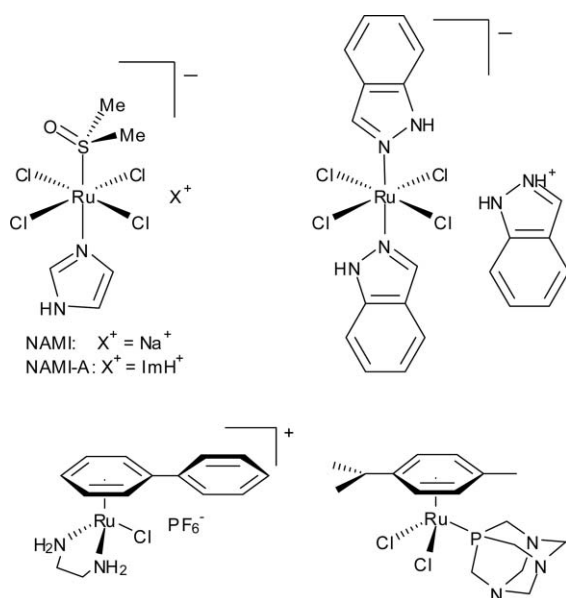


Fig. 1 Schematic structures of some of the most promising and thoroughly investigated anticancer Ru compounds: NAMI-A (top-left), KP1019 (top-right), RM175 (bottom-left), and RAPTA-C (bottom-right).

Both compounds are moderately cytotoxic *in vitro* and, in animal models, have activities different from established Pt drugs: NAMI-A was found to be particularly active against the development and growth of metastases of solid tumours,¹¹ whereas KP1019 showed excellent activity against platinum-resistant colorectal tumours.¹²

In more recent years new classes of cationic and neutral half-sandwich Ru(II)-arene compounds, developed by the groups of Sadler and of Dyson,^{13,14} were found to have promising *in vitro* and *in vivo* anticancer activity. Representative examples of these organometallic compounds (also called *piano-stool* compounds) are $[(\eta^6\text{-biphenyl})\text{Ru}(\text{en})\text{Cl}][\text{PF}_6^-]$ (RM175, en = ethane-1,2-diamine) and $[(\eta^6\text{-}p\text{-cymene})\text{RuCl}_2(\text{pta})]$ (RAPTA-C, pta = 1,3,5-triaza-7-phosphatricyclo[3.3.1]decane) (Fig. 1). In general, Ru compounds have a lower toxicity compared to Pt drugs.

For the reasons mentioned above, it is therefore of great interest to investigate the anticancer properties of porphyrin-ruthenium conjugates. Indeed, very recently, Therrien and co-workers re-

ported that neutral conjugates of *meso*-pyridylporphyrins with organometallic $[\text{Ru}(\eta^6\text{-arene})\text{Cl}_2]$ fragments, that are moderately cytotoxic in the dark against Me300 human melanoma cells, become cytotoxic upon irradiation with visible light.¹⁵

In addition to potential PDT activity, in porphyrin-metal conjugates the excitation of the chromophore with visible light might induce photoreactivity in the peripheral metal fragment(s). A particularly attractive target is the photochemical delivery of NO from metal-nitrosyls that would offer a mean for promoting NO-induced apoptosis (programmed cell-death) in cancer cells under the control of visible light. To this regard, Mascharak and co-workers showed that photo-induced release of NO with visible light can be obtained by conjugation of Ru-nitrosyls to light-harvesting chromophores,¹⁶ whereas Ford and co-workers reported that the conjugate of protoporphyrin IX with an iron-sulfur-nitrosyl cluster is an efficient photo-inducible NO donor upon irradiation with low-energy light.¹⁷ With this purpose, we recently prepared and structurally characterized several conjugates of *meso*-4'-pyridylporphyrins with ruthenium-nitrosyl complexes, including the water soluble tetraruthenated derivative of zinc *meso*-4'-tetrapyrrolylporphyrin (Zn-4'TPP), $\text{Na}_4[\text{Zn-4'TPP}\{\text{RuCl}_4(\text{NO})\}_4]$, in which each pyridyl N atom is bound to a $[\text{RuCl}_4(\text{NO})]^-$ fragment.¹⁸

Beside to ruthenium compounds that have one or more substitutionally labile ligands, *i.e.* that are expected to open up coordination positions *in vivo* allowing direct coordination to biological targets (*functional compounds*), porphyrins can also be conjugated to peripheral ruthenium fragments that are coordinatively saturated and substitutionally inert (*structural compounds*).¹⁹ For reasons more clearly detailed in the Discussion, also such water-soluble porphyrin conjugates are worth being investigated in a biomedical context, in particular as telomerase inhibitors and K⁺ channel blockers.

Conjugation strategies

The coordination of a porphyrin to peripheral metal fragments can occur either through a single bond or through multiple bonds (*i.e.* through a chelating moiety). Typically, pyridyl rings are used as peripheral ligands for the coordination of late transition metal ions.²⁰⁻²² ‡ The former synthetic approach has an indubitable advantage: the commercially available, or otherwise easily prepared, *meso*-pyridylporphyrins (PyPs) can be exploited. In PyPs, the pyridyl N atoms can be either in 3' (3'PyPs) or, more commonly, in 4' positions (4'PyPs). Even though synthetically more demanding, also PyPs in which the pyridyl rings are not directly bound at the *meso* positions, but are connected through a spacer, have been used occasionally.²³ In the case of ruthenium, the vast majority of the conjugates reported in the literature involve the symmetrical coordination of four equal Ru fragments to a *meso*-tetrapyrrolylporphyrin (TPyP).²⁴⁻²⁶ Aside from the already mentioned compounds made by us¹⁸ and by Therrien and co-workers,¹⁵ relatively few TPyP-(Ru)₄ conjugates were explicitly prepared for biomedical investigations. In such context, the peripheral Ru fragments were typically of the type $\text{Ru}(\text{chel})_2\text{X}$,

‡ Porphyrins bearing peripheral organometallic fragments at *meso* or β positions have been recently reviewed: B. M. J. M. Suijkerbuijk and R. J. M. Klein Gebbink, *Angew. Chem., Int. Ed.*, 2008, **47**, 7396.

where chel is a polypyridyl ligand.^{27,28} The choice of ruthenium-polypyridyl complexes was motivated by two main reasons: (i) they have a good affinity for DNA.²⁹ Thus, similarly to Pt(II) fragments, they might behave as chaperones and help localizing the porphyrin photosensitizer close to DNA where the photoinduced generation of ROS would be more effective for inducing cell damage. (ii) They are potential photosensitizers, and some of them were found capable of DNA photooxidation and photocleavage.^{27,30,31}

Examples of mono- and di-pyridylporphyrins conjugated to Ru-polypyridyl fragments were also recently reported and their DNA binding properties and photocleavage capability described.^{32–34} The residual *meso*-phenyl groups may be exploited for increasing water solubility (*e.g.* through appropriate substituents) or for enhancing the photophysical properties (*e.g.* by fluorination). Some fluorinated porphyrins bearing one or two peripheral [Ru(bpy)₂Cl]⁺ fragments were also found to induce apoptosis in melanoma skin cells upon irradiation in the visible range (PDT activity).^{32,34}

Nevertheless, the single-bond conjugates might be insufficiently stable towards aquation under *in vivo* conditions, with consequent loss of the peripheral Ru fragments. Conjugation through multiple bonds increases the stability of the adducts but poses the necessity of developing affordable synthetic strategies towards porphyrins with peripheral chelating moieties. Even though a few examples of such Ru-porphyrin conjugates are known in the literature, we are unaware that any of them was explicitly prepared and investigated for biomedical purposes so far.

Herein, we describe Ru-porphyrin conjugates whose total charge varies from –4 to +8. Beside several conjugates with pyridylporphyrins, we describe the preparation in acceptable yields of a series of porphyrins that bear from 1 to 4 peripheral bipyridine moieties (*meso*-(*p*-bpy-phenyl)porphyrins, bpy_{*n*}-PPs, *n* = 1–4) and their use for the coordination of ruthenium fragments.

Experimental

Mono and bidimensional (H–H COSY, NOESY, ROESY, and HSQC) ¹H NMR spectra were recorded at 400 or 500 MHz on a JEOL Eclipse 400FT or on a Varian 500 spectrometer, respectively. All spectra were run at ambient temperature, unless otherwise stated. ¹H chemical shifts in D₂O were referenced to the internal standard 2,2-dimethyl-2,2-silapentane-5-sulfonate (DSS) at δ = 0.00. In other solvents chemical shifts were referenced to the peak of residual non-deuterated solvent (δ = 7.26 for CDCl₃, 4.33 for CD₃NO₂, 3.31 for CD₃OD, 2.50 for DMSO-*d*₆, 1.73 for THF-*d*₈). UV-vis spectra were obtained at *T* = 25 °C on a Jasco V-500 UV-vis spectrophotometer equipped with a Peltier temperature controller, using 1.0 cm path-length quartz cuvettes (3.0 mL). Infrared spectra were recorded on a Perkin-Elmer 983G spectrometer. Electrospray mass spectra were recorded in the positive ion mode on a Bruker Esquire ESI-MS instrument. Fluorescence spectra were recorded on a F-4550 Hitachi spectrofluorimeter.

Meso-tetra(*p*-aminophenyl)porphyrin (*p*(NH₂)₄PP) was purchased from TCI-Europe. 4-methyl-2,2'-bipyridine-4'-carboxylic acid (bpyAc),³⁵ [nBu₄N][*trans*-RuCl₄(*dms*o-S)₂],³⁶ [Ru([9]aneS3)(*dms*o)₃][CF₃SO₃]₂,³⁷ [Ru([9]aneS3)(*en*)Cl][CF₃SO₃],³⁸ [Ru([9]aneS3)(bpy)(*dms*o-S)][CF₃SO₃],³⁸ [Ru([9]aneS3)(bpyAc)(*dms*o-S)][CF₃SO₃]₂ (**10**),³⁹ [Ru([12]aneS4)(*dms*o-S)Cl][Cl],⁴⁰ [Ru([12]aneS4)(*dms*o-S)(H₂O)][CF₃SO₃]₂,⁴¹ and [Ru([12]aneS4-

(*dms*o-S)(NO₃)] [NO₃]⁴¹ were prepared according to the published procedures.

The Ru-porphyrin conjugates precipitate with variable amounts of crystallization solvent, that depend on the batch. For this reason elemental analysis of such conjugates did not afford reliable and reproducible results and—aside for complex **12**—the values are not reported here (typically, some of the elemental analysis values, especially for C, differ from calculated values by > 0.5%). Nevertheless, the proposed formulas are all consistent with the ¹H NMR and ESI spectra, and (for conjugate **4**) with X-ray crystallographic analysis.

Synthesis of porphyrins

5-(4'-Pyridyl)-10,15,20-tris(4'-carboxyphenyl)porphyrin (4'-MPyCbPP). As previously described by us, 4'-MPyCbPP was obtained by hydrolysis of the ester groups of 5-(4'-pyridyl)-10,15,20-tris(4'-carboxymethylphenyl)porphyrin (4'-MPyCbMePP) under basic conditions in THF–methanol mixtures.⁴²

***Meso*-(*p*-nitrophenyl)porphyrins *p*(NO₂)_{*n*}PP (*n* = 1–3) and *meso*-(*p*-aminophenyl)porphyrins *p*(NH₂)_{*n*}PP (*n* = 1–3)**. 5-(*p*-nitrophenyl)-10,15,20-triphenylporphyrin (*p*(NO₂)PP), 5,15-bis(*p*-nitrophenyl)-10,20-diphenylporphyrin (*p*(NO₂)₂*trans*-PP), 5,10-bis(*p*-nitrophenyl)-15,20-diphenylporphyrin (*p*(NO₂)₂*cis*-PP), and 5,10,15-tris(*p*-nitrophenyl)-20-phenylporphyrin (*p*(NO₂)₃PP) were prepared by regioselective nitration of the phenyl groups of *meso*-tetraphenylporphyrin using NaNO₂ and TFA, as reported in the literature.⁴³ The crude products were characterized by ¹H NMR spectroscopy and then reduced to the corresponding aminophenyl-porphyrins using standard SnCl₂–HCl conditions.^{43,44} The aminophenyl-porphyrins (*p*(NH₂)PP, *p*(NH₂)₂*trans*-PP, *p*(NH₂)₂*cis*-PP, and *p*(NH₂)₃PP) were obtained in pure form by column chromatography on silica gel eluted with CHCl₃–EtOH or CHCl₃–MeOH mixtures (see below). All compounds gave ¹H NMR and UV-vis spectra (ESI)[†] consistent with those reported in the literature.

***Meso*-(*p*-bpy-phenyl)porphyrins (bpy_{*n*}-PPs)**. The *meso*-phenylporphyrins peripherally substituted with bipyridyl groups—*meso*-(*p*-bpy-phenyl)porphyrins (bpy_{*n*}-PP, *n* = 1–4)—were prepared by direct coupling of the *meso*-(*p*-aminophenyl)porphyrins with bpyAc. The reactions were carried out in pyridine using 1 equiv. of *N*-(3-dimethylaminopropyl)-*N'*-ethylcarbodiimide hydrochloride (EDCI) as coupling agent and 2 equiv. of bpyAc for each aminophenyl group. The general procedure is described in detail only for bpy-PP.

5-[4-(4-Methyl-2,2'-bipyridine-4'-carboxamidyl)phenyl]-10,15,20-triphenylporphyrin (bpy-PP). A 81.6 mg amount of bpyAc (0.38 mmol) and 72.9 mg of EDCI (0.38 mmol) were dissolved in 6 mL of pyridine. The solution was stirred for 10 min, then a 120 mg amount of *p*(NH₂)PP (0.19 mmol) was added and stirring was continued at r.t. The reaction was monitored by TLC (silica gel, CHCl₃–EtOH 90 : 10). After 1 h, water (20 mL) was added to the reaction mixture. The purple precipitate was removed by filtration, washed with water (80 mL) and vacuum dried at r.t. The solid was purified on a plug of silica gel eluting with CHCl₃ for removal of residual *p*(NH₂)PP and then with CHCl₃–EtOH 85 :

15 for recovering the product. Removal of solvent yielded 129 mg (82%) of the title compound.

δ_{H} (CDCl₃): -2.78 (br, 2 H, NH), 2.51 (s, 3 H, CH₃), 7.24 (d, 1 H, H5'), 7.77 (m, 9 H *p* + *mPh*), 8.03 (d, *J* = 4.8 Hz, 1 H, H5), 8.14 (d, 2 H, *J* = 8.4, *mbg*), 8.27 (m, 8 H, *oPh* + *obg*), 8.37 (s, 1 H, H3'), 8.61 (d, 1 H, *J* = 4.9 Hz, H6'), 8.68 (s, 1 H, H3), 8.84 (m, 6 H, βH), 8.94 (d, 2 H, βH), 8.95 (d, 1 H, *J* = 4.9 Hz, H6); δ_{H} (THF-*d*₆): -2.79 (br, 2 H, NH), 2.32 (s, 3 H, CH₃), 7.09 (d, *J* = 4.2 Hz, 1 H, H5'), 7.64 (m, 9 H *p* + *mPh*), 7.82 (d, *J* = 4.4 Hz, 1 H, H5), 8.09 (m, 8 H, *oPh* + *mbg*), 8.18 (d, *J* = 8.1 Hz, 2 H, *obg*), 8.33 (s, 1 H, *bipy* H3'), 8.42 (d, *J* = 4.8 Hz, 1 H, H6'), 8.70 (m, 8 H, βH), 8.80 (d, *J* = 4.2 Hz, 1 H, H6), 8.99 (s, 1 H, H3), 10.17 (s, 1 H, CONH). UV-vis λ_{max} (CHCl₃)/nm ($\epsilon \times 10^{-3}/\text{dm}^3 \text{ mol}^{-1} \text{ cm}^{-1}$): 420 (470), 516 (19.7), 551 (11), 590 (8.0), 648 (6.7). ESI-MS: *m/z* 826.4 [MH⁺].

5,10-Bis[4-(4-methyl-2,2'-bipyridine-4'-carboxyamidyl)phenyl]-15,20-diphenylporphyrin (bpy₂-*cis*PP). Same procedure as for bpy-PP, with the following parameters: bpyAc (53.1 mg, 0.24 mmol); EDCI (47.5 mg, 0.24 mmol); *p*(NH₂)₂-*cis*-PP (40 mg, 0.062 mmol); pyridine (4 mL); reaction time (1.5 h). Yield: 42 mg (65%).

δ_{H} (CDCl₃): -2.77 (br, 2 H, NH), 2.50 (s, 6 H, CH₃), 7.24 (d, 2 H, H5'), 7.76 (m, 6 H, *m* + *pPh*), 8.02 (d, 2 H, *J* = 5.1 Hz, H5), 8.12 (d, 4 H, *J* = 8.4 Hz, *mbg*), 8.21–8.27 (m, 8 H *obg* + *oPh*), 8.36 (s, 2 H, H3'), 8.62 (d, 2 H, *J* = 4.9 Hz, H6'), 8.75 (s, 2 H, H3), 8.84–8.93 (m, 10 H, βH + H6). UV-vis λ_{max} (CHCl₃)/nm ($\epsilon \times 10^{-3}/\text{dm}^3 \text{ mol}^{-1} \text{ cm}^{-1}$): 421 (409), 517 (21.1), 553 (12.5), 591 (8.4), 647 (7.4).

5,15-Bis[4-(4-methyl-2,2'-bipyridine-4'-carboxyamidyl)phenyl]-10,20-diphenylporphyrin (bpy₂-*trans*PP). Same procedure as for bpy-PP, with the following parameters: bpyAc (13.7 mg, 0.064 mmol); EDCI (12.2 mg, 0.064 mmol); *p*(NH₂)₂-*trans*-PP (10 mg, 0.016 mmol); pyridine (2 mL); reaction time (1.5 h). After addition of water (10 mL), the product was extracted with chloroform (4 × 20 mL). The organic layer was then evaporated to dryness and the purple residue (11 mg) purified on a column of silica gel eluted first with CHCl₃ followed by CHCl₃-MeOH 95 : 5. Yield: 3 mg (18%).

δ_{H} (CDCl₃): -2.77 (br s, 2 H, NH), 2.50 (s, 3 H CH₃), 7.24 (d, 2 H, H5'), 7.76 (m, 6 H *p* + *mPh*), 8.01 (d, *J* = 4.8 Hz, 2 H, H5), 8.12 (d, *J* = 8.4 Hz, 4 H, *mbg*), 8.20–8.27 (m, 8 H, *obg* + *oPh*), 8.36 (s, 2 H, H3'), 8.60 (d, 2 H, *J* = 4.9 Hz, H6'), 8.81 (s, 2 H, H3), 8.86–8.94 (m, 10 H, βH + H6).

5,10,15-Tris[4-(4-methyl-2,2'-bipyridine-4'-carboxyamidyl)phenyl]-20-phenylporphyrin (bpy₃-PP). Same procedure as for bpy-PP, with the following parameters: bpyAc (88.2 mg, 0.46 mmol); EDCI (87.4 mg, 0.46 mmol); *p*(NH₂)₃PP (50 mg, 0.077 mmol); pyridine (7 mL); reaction time (1.5 h). After addition of water (10 mL), the product was extracted with chloroform (4 × 20 mL). Yield: 69 mg (73%).

δ_{H} (CDCl₃): -2.77 (br s, 2 H, NH), 2.50 (s, 9 H, CH₃), 7.24 (d, 3 H, H5'), 7.76 (m, 3 H, *m* + *pPh*), 8.01 (d, 3 H, *J* = 4.6 Hz, H5), 8.12 (d, 6 H, *J* = 8.3 Hz, *mbg*), 8.23 (m, 8 H, *obg* + *oPh*), 8.35 (s, 3 H, H3'), 8.60 (d, 3 H, *J* = 5.0, H6'), 8.75 (s, 3 H, H3), 8.86 (d, 3 H, H6), 8.90 (m, 2 H, βH), 8.93 (m, 6 H, βH). UV-vis λ_{max} (CHCl₃)/nm ($\epsilon \times 10^{-3}/\text{dm}^3 \text{ mol}^{-1} \text{ cm}^{-1}$): 423 (450), 518 (21.0), 554

(14.0), 592 (9.0), 648 (7.9). ESI-MS: *m/z* 1248.5 [MH⁺]; 1270.5 [M + Na⁺].

5,10,15,20-Tetrakis[4-(4-methyl-2,2'-bipyridine-4'-carboxyamidyl)phenyl]porphyrin (bpy₄-PP). Same procedure as for bpy-PP, with the following parameters: bpyAc (42.0 mg, 0.196 mmol); EDCI (52.0 mg, 0.267 mmol); *p*(NH₂)₄PP (30 mg, 0.045 mmol); pyridine (4 mL); reaction time (3 h). Yield: 60 mg (91%).

δ_{H} (CDCl₃): -2.76 (br s, 2 H, NH), 2.52 (s, 12 H, CH₃), 7.26 (d, 4 H, H5' overlapped with the resonance of residual CHCl₃), 8.03 (d, 4 H, *J* = 0.7, 4.1 Hz, H5), 8.13 (d, 8 H, *J* = 8.3 Hz, *mbg*), 8.28 (m, 8 H, *J* = 8.2 Hz *obg*), 8.38 (s, 4 H, H3'), 8.55 (s, 4 H, H3), 8.64 (d, 4 H, *J* = 5.0, H6'), 8.95 (m, 12 H, βH + H6). UV-vis λ_{max} (CHCl₃)/nm: 424, 518, 556, 594, 651. ESI-MS: *m/z* 1481.5 [M + Na⁺].

Synthesis of complexes and porphyrin conjugates

[Na]₄[4'TPyP{*trans*-RuCl₄(*dms*o-S)}₄]₄ (2). A 119 mg amount of sodium tetraphenylborate (0.34 mmol) dissolved in 2 mL of nitromethane was added to a solution of **1** (50 mg, 0.017 mmol) in 1 mL of nitromethane. The precipitate that formed immediately was collected by filtration, washed with acetone and diethyl ether and dried under vacuum at r.t. Yield: 34.6 mg (97%).

Selected δ_{H} (D₂O): -13.0 (v br, *dms*o-S). UV-vis λ_{max} (H₂O)/nm (relative intensity): 414 (100), 515 (5.6), 550 (1.7), 580 (2.0), 634 (0.5).

[4'TPyP{Ru(9]aneS3(en)}₄][CF₃SO₃]₈ (3). A 46.5 mg amount of [Ru(9]aneS3(en)Cl](CF₃SO₃) (0.14 mmol) dissolved in 2 mL of MeOH was added to a suspension of 4'TPyP (20 mg, 0.032 mmol) in 15 mL of CHCl₃. After addition of AgCF₃SO₃ (35.7 mg, 0.14 mmol), the reaction mixture was heated to reflux for 4 h. The reaction was monitored by TLC analysis (silica gel, CH₂Cl₂-EtOH 90 : 10). The dark solution was concentrated *in vacuo* to ca. 10 mL and a few drops of diethyl ether were added. A purple solid formed upon standing, which was removed by filtration and vacuum dried. The solid was redissolved in 10 mL of MeOH and centrifuged to eliminate AgCl. The solution was evaporated to dryness under reduced pressure to obtain the title compound. Yield 59 mg (92%).

δ_{H} (D₂O): 2.6–3.1 (m, 64 H, CH₂ [9]aneS3 + en), 4.17 (m, 8 H, NH₂), 5.09 (m, 8 H, NH₂), 8.52 (d, 8 H, *J* = 5.67, H3,5), 9.11 (v br s, 8 H, βH), 9.36 (d, 8 H, *J* = 5.71, H2,6). δ_{H} (CD₃OD, 25 °C): 2.5–3.1 (m, 64 H, [9]aneS3 + en), 4.38 (br m, 8 H, NH₂), 5.32 (m, 8 H, NH₂), 8.42 (d, 8 H, *J* = 6.48, H3,5), 9.04 (v br, 8 H, βH), 9.33 (d, 8 H, *J* = 6.34, H2,6). δ_{H} (CD₃OD, -15 °C): 2.5–3.1 (m, 64 H, [9]aneS3 + en), 4.46 (m, 8 H, NH₂), 5.43 (m, 8 H, NH₂), 8.42 (d, 8 H, *J* = 6.21, H3,5), 8.97 (s, 4 H, βH), 9.30 (s, 4 H, βH), 9.34 (d, 8 H, *J* = 6.18, H2,6). UV-vis λ_{max} (CH₃OH)/nm (relative intensity (%)): 419 (100), 513 (7.7), 549 (4.0), 589 (2.8), 646 (1.8).

[4'TPyP{Ru(9]aneS3(bpy)}₄][CF₃SO₃]₈ (4). A 90.0 mg amount of [Ru(9]aneS3)(bpy)(*dms*o-S)](CF₃SO₃)₂ (0.11 mmol) dissolved in 2 mL of methanol was added to a suspension of 4'TPyP (15.5 mg, 0.025 mmol) in 15 mL of CHCl₃. The mixture was heated to reflux for 8 h, until disappearance of the spot of unreacted porphyrin according to TLC analysis (silica gel, CHCl₃-EtOH 90 : 10). Dropwise addition of diethyl ether to the solution induced the precipitation of a purple solid, that was removed by filtration and washed with diethyl ether and dried under vacuum

at r.t. The solid, that according to ^1H NMR spectroscopic analysis contained unreacted Ru complex, was recrystallized twice from nitromethane/diethyl ether. Yield: 64 mg (71%).

δ_{H} (CD_3NO_2 , see ESI† for labelling scheme): -3.35 (s, 2 H, NH), 3.5–2.7 (m, 48 H, CH_2 [9]aneS3), 7.92 (t, 8 H, H5,5'), 8.13 (d, 8 H, H3,5), 8.33 (t, 2 H, H4,4'), 8.63 (m, 16 H, $\beta\text{H} + \text{H}2,6$), 9.22 (d, 2 H, H3,3'), 9.48 (d, 2 H, H6,6'). UV-vis λ_{max} (CH_3NO_2)/nm (relative intensity (%)): 425 (100), 518 (8.8), 553 (5.4), 590 (4.2), 646 (2.8).

[nBu₄N][trans-RuCl₄(dmsO-S)(4'-MPyCbPP)]. A 129 mg amount of [nBu₄N][trans-RuCl₄(dmsO-S)₂] (0.20 mmol) was added to a solution of 4'-MPyCbPP (50 mg, 0.067 mmol) in THF (10 mL) containing 200 μL of DMSO. After 24 h at ambient temperature, dropwise addition of diethyl ether afforded a purple precipitate that was removed by filtration, washed with chloroform and diethyl ether and dried under vacuum at room temperature. Yield: 74 mg (83%).

Selected δ_{H} (CD_3OD): -13.0 (v br, dmsO-S), -1.1 and 5.7 (br, H2,6 and H3,5), 7.8 and 8.2 (m, oPh + mH + βH), 8.5 (br, βH). UV-vis λ_{max} (CH_2Cl_2)/nm ($\epsilon \times 10^{-3}/\text{dm}^3 \text{ mol}^{-1} \text{ cm}^{-1}$): 416 (513), 513 (25), 547 (12) 589 (7.7), 644 (5.3). Selected IR (KBr) $\nu_{\text{max}}/\text{cm}^{-1}$ 3315 (m, NH), 1119 (s, S=O).

Na[trans-RuCl₄(dmsO-S)(4'-MPyCbPP)] (5). A 50.0 mg amount of Na[B(C₆H₅)₄] (0.15 mmol) was added to a solution of [nBu₄N][trans-RuCl₄(dmsO-S)(MPyCbPP)] (50.0 mg, 0.037 mmol) in acetone (20 mL) containing 50 μL of DMSO. Dropwise addition of diethyl ether (10 mL) induced the precipitation of a purple solid, that was removed by filtration, washed with nitromethane and diethyl ether and dried under vacuum at room temperature. Yield: 39.5 mg (95%).

δ_{H} ($\text{DMSO}-d_6$): -12.7 (v br, dmsO-S), -4.0 (br, NH), -0.8 and 5.8 (br, H2,6 and H3,5), 8.13 and 8.55 (m, oPh + mH + βH), 13.2 (s, COOH). UV-vis λ_{max} (acetone)/nm ($\epsilon \times 10^{-3}/\text{dm}^3 \text{ mol}^{-1} \text{ cm}^{-1}$): 416 (273), 513 (15), 547 (7), 589 (5), 645 (4).

[Bpy-PP{Ru(9]aneS3)(dmsO-S)}][CF₃SO₃]₂ (6). A 33.5 mg amount of Bpy-PP (0.041 mmol) and 30 mg of [Ru(9]aneS3)(dmsO)₃][CF₃SO₃]₂ (0.036 mmol) were added to a CHCl_3 - CH_3NO_2 (1 : 3) mixture (12 mL). The solution was stirred at r.t. and monitored by TLC (alumina plates, CHCl_3 -MeOH 90 : 10). After 24 h it was evaporated to dryness under vacuum, and the solid residue redissolved in CHCl_3 (5 mL). Dropwise addition of diethyl ether to the purple-brown solution induced the precipitation of a purple solid, that was removed by filtration and washed repeatedly with diethyl ether and dried under vacuum at r.t. Yield: 40 mg (72%).

δ_{H} (CD_3NO_2): -2.81 (br, 2 H, NH), 2.74 (s, 3 H, CH₃), 2.81 (s, 3 H, CH₃ dmsO-S), 2.88 (s, 3 H, CH₃ dmsO-S), 2.53–3.41 (m, 12 H, CH₂ [9]aneS3), 7.77 (d, 1 H, $J = 5.6$ Hz, H5'), 7.87 (br m, 9 H $m + p\text{Ph}$), 8.30 (br m, 11 H, oPh + mbg + obg + H5), 8.74 (s, 1 H, H3'), 8.97 (9 H, $\beta\text{H} + \text{H}6'$), 9.12 (s, 1 H, H3), 9.33 (d, $J = 5.3$ Hz, 1 H, H6), 9.75 (s, 1 H, CONH). δ_{H} (CD_2Cl_2): -2.86 (br, 2 H, NH), 2.63 (s, 3 H, CH₃), 2.67 (s, 3 H, CH₃ dmsO-S), 2.85 (s, 3 H, CH₃ dmsO-S), 2.26–3.36 (m, 12 H, CH₂ [9]aneS3), 7.56 (d, 1 H, $J = 5.3$ Hz, H5'), 7.76 (br m, 9 H $m + p\text{Ph}$), 8.24 (br m, 11 H, oPh + mbg + obg + H5), 8.53 (s, 1 H, H3'), 8.70 (d, 1 H, $J = 5.2$ Hz, H6'), 8.85–8.92 (m, 10 H, $\beta\text{H} + \text{H}3 + \text{H}6$), 10.61 (s, 1 H, CONH). UV-vis λ_{max} (CHCl_3)/nm ($\epsilon \times 10^{-3}/\text{dm}^3 \text{ mol}^{-1} \text{ cm}^{-1}$): 420

(368), 516 (19), 552 (13), 591 (97), 647 (92). ESI-MS: m/z 1256.1 [{Bpy-PP}{Ru(9]aneS3)(CF₃SO₃)}]⁺.

[Bpy₂-cisPP{Ru(9]aneS3)(dmsO-S)}][CF₃SO₃]₄ (7). A 17.6 mg amount of Bpy₂-cisPP (0.017 mmol) dissolved in 2 mL of CHCl_3 was added to a solution of [Ru(9]aneS3)(dmsO)₃][CF₃SO₃]₂ (30.0 mg, 0.036 mmol) dissolved in 5 mL of acetone. The resulting solution was heated to reflux for 5 h, during which time a purple sticky precipitate formed. After decanting the solution, the solid was washed with diethyl ether and dried under vacuum. A second fraction of solid product (that was treated as above) was obtained upon dropwise addition of diethyl ether to the mother liquor. Total yield: 22 mg (55%).

δ_{H} (CD_3NO_2): -2.83 (br s, 2H, NH), 2.74 (s, 6H, CH₃), 2.80 (s, 6H, dmsO-S), 2.89 (s, 6H, CH₃ dmsO-S), 2.6–3.45 (m, 24H, CH₂ [9]aneS3), 7.74 (d, 2H, $J = 4.8$ Hz, H5'), 7.87 (m, 6H, $m + p\text{Ph}$), 8.37 (m, 14H, mbg + obg + oPh + H5), 8.76 (s, 2H, H3'), 8.98 (m, 10H, $\beta\text{H} + \text{H}6'$), 9.16 (s, 2H, H3), 9.31 (d, 2H, $J = 5.8$ Hz, H6), 10.04 (s, 2H, CONH). δ_{H} (acetone- d_6): -2.70 (br, 2H, NH), 2.74 (s, 6H, CH₃), 2.90 (s, 6H, dmsO-S), 3.03 (s, 6H, dmsO-S), 2.74–3.55 (m, 24H, CH₂ [9]aneS3), 7.86 (m, 8H, $p + m\text{Ph} + \text{H}5'$), 8.37 (m, 12H, mbg + obg + oPh), 8.39 (d, $J = 5.9$ Hz, 2H, H5), 8.91 (m, 8H, βH), 9.02 (s, 2H, H3'), 9.18 (d, $J = 5.9$ Hz, 2H, H6'), 9.30 (s, 2H, H3), 9.46 (d, $J = 5.6$ Hz, 2H, H6), 10.73 (s, 2H, CONH). UV-Vis λ_{max} (acetone)/nm ($\epsilon \times 10^{-3}/\text{dm}^3 \text{ mol}^{-1} \text{ cm}^{-1}$): 419 (184), 514 (19.9), 549 (13.9), 591 (9.2), 647 (8.8). ESI-MS: m/z 947.4 [{bpy₂-cisPP}{Ru(9]aneS3)(CF₃SO₃)₂}]²⁺.

[Bpy₃-PP{Ru(9]aneS3)(dmsO-S)}][CF₃SO₃]₆ (8). A 20.0 mg amount of bpy₃-PP (0.016 mmol) dissolved in 2.5 mL of CHCl_3 was added to a solution of [Ru(9]aneS3)(dmsO)₃][CF₃SO₃]₂ (43.0 mg, 0.053 mmol) dissolved in 7 mL of acetone. The resulting solution was heated to reflux for 24 h, during which time a purple sticky precipitate formed. After decanting the solution, it was washed with diethyl ether and dried under vacuum. Yield: 30 mg (58%).

δ_{H} (CD_3NO_2): -2.77 (br s, 2 H, NH), 2.75 (s, 9 H CH₃), 2.81 (s, 9 H, dmsO-S), 2.89 (s, 9 H, dmsO-S), 2.65–3.47 (m, 24 H, CH₂ [9]aneS3), 7.78 (d, 3 H, $J = 5.6$ Hz, H5'), 7.89 (m, 3 H, $m + p\text{Ph}$), 8.38 (m, 17 H, oPh + H5 + mbg + obg), 8.76 (s, 3 H, H3'), 8.99 (d, 3 H, $J = 5.7$ Hz, H6), 9.07 (m, 8 H, βH), 9.15 (s, 3 H, H3), 9.34 (d, 3 H, $J = 5.8$ Hz, H6), 9.92 (s, 2 H, CONH), 9.99 (s, 1 H, CONH). UV-vis λ_{max} (CH_3NO_2)/nm ($\epsilon \times 10^{-3}/\text{dm}^3 \text{ mol}^{-1} \text{ cm}^{-1}$): 421 (386), 517 (24), 553 (19), 591 (12), 647 (12). ESI-MS: m/z 846.8 [{bpy₃-PP}{Ru(9]aneS3)(CF₃SO₃)₃}]³⁺.

Bpy₄-PP{Ru(9]aneS3)(dmsO-S)}][CF₃SO₃]₈ (9). A 20.0 mg amount of bpy₄-PP (0.014 mmol) dissolved in 10 mL of CHCl_3 was added to a solution of [Ru(9]aneS3)(dmsO)₃][CF₃SO₃]₂ (47.5 mg, 0.058 mmol) dissolved in 45 mL of acetone. The resulting solution was heated to reflux for 2 h, during which time a purple precipitate formed. The solution was concentrated under vacuum to ca. 15 mL. The solid was removed by filtration, washed with diethyl ether and dried under vacuum. Yield: 46 mg (81%).

δ_{H} (CD_3NO_2): -2.72 (br s, 2 H, NH), 2.75 (s, 12 H, CH₃), 2.81 (s, 12 H, dmsO-S), 2.89 (s, 12 H, dmsO-S), 2.65–3.50 (m, 12 H, CH₂ [9]aneS3), 7.76 (d, 4 H, $J = 5.4$ Hz, H5'), 8.35 (m, 20 H, H5 + mbg + obg), 8.75 (s, 4 H, H3'), 8.98 (d, 4 H, $J = 5.8$ Hz, H6'), 9.08 (m, 8 H, βH), 9.13 (s, 4 H, H3), 9.33 (d, 4 H, $J = 5.6$ Hz, H6), 9.92

(br s, 4 H, CONH). UV-vis λ_{max} (DMSO)/nm (relative intensity (%)): 424 (100), 519 (5.9), 557 (4.8), 593 (2.1), 651 (2.6).

[Bpy₄-PP{Ru([12]aneS4)}₄][CF₃SO₃]₈ (11). To a 15.0 mg amount of bpy₄-PP (0.010 mmol) dissolved in 8 mL of CHCl₃ a solution of [Ru([12]aneS4)(dmsO-S)(H₂O)][CF₃SO₃]₂ (32.2 mg, 0.044 mmol) dissolved in 35 mL of methanol was added. The resulting solution was heated to reflux for 36 h (the reaction was monitored by TLC, silica plates, CHCl₃-EtOH 9 : 1), during which time a fine purple precipitate formed. The suspension was concentrated under vacuum to *ca.* 15 mL and diethyl ether (*ca.* 3 mL) was added dropwise to increase the amount of precipitate. The solid was removed by filtration, washed with diethyl ether and dried under vacuum. Yield: 19 mg (67%).

δ_{H} (CD₃NO₂): -2.72 (br s, 2 H, NH), 2.73 (s, 12 H, CH₃), 2.80–4.00 (m, 16 H, CH₂ [12]aneS4), 7.66 (d, 4 H, *J* = 5.4 Hz, H5'), 8.36 (m, 20 H, H5 + *mbg* + *obg*), 8.77 (s, 4 H, H3'), 9.00–9.20 (m, 12 H, β H + H3), 9.35 (br m, 4 H, H6'), 9.74 (br m, 8 H, CONH + H6). δ_{H} (acetone-*d*₆): -2.65 (br s, 2 H, NH), 2.71 (s, 12 H CH₃), 2.80–4.00 (m, 16 H, CH₂ [12]aneS4), 7.72 (d, 4 H, *J* = 6.1 Hz, H5'), 8.37 (m, 20 H, H5 + *mbg* + *obg*), 9.00 (m, 12 H, H3' + β H), 9.35 (s, 4 H, H3), 9.47 (br m, 4 H, H6') 9.83 (br m, 4 H, H6), 10.67 (s, 4 H, CONH). δ_{H} (acetone-*d*₆, *T* = -60 °C): -2.65 (br s, 2 H, NH), 2.69 (s, 12 H CH₃), 2.80–4.00 (m, 16 H, CH₂ [12]aneS4), 7.77 (d, 4 H, *J* = 5.9 Hz, H5'), 8.40 (m, 20 H, *J* = 5.8 Hz, H5 + *mbg* + *obg*), 8.90 (s, 4 H, β H), 9.06 (s, 4 H, H3'), 9.19 (s, 4 H, β H), 9.41 (s, 4 H, H3'), 9.53 (d, 4 H, *J* = 6.0 Hz H6'), 9.90 (d, 4 H, *J* = 5.9 Hz, H6), 10.91 (s, 4 H, CONH). UV-vis λ_{max} (CH₃NO₂)/nm (relative intensity (%)): 423 (100), 518 (5.8), 556 (4.3), 593 (2.1), 649 (2.5).

[Ru([12]aneS4)(bpyAc)][CF₃SO₃]₂ (12). A 30 mg amount of [Ru([12]aneS4)(dmsO-S)(H₂O)][CF₃SO₃]₂ (0.041 mmol) was partially dissolved in acetone (15 mL) and heated to reflux. Upon complete dissolution of the complex, a 8.73 mg amount of bpyAc (0.041 mmol) was added and the solution was refluxed for 2 h and then concentrated under vacuum to *ca.* 5 mL. Dropwise addition of diethyl ether (*ca.* 3 mL) induced the formation of a precipitate, that was removed by filtration, washed with diethyl ether and dried under vacuum. Yield: 8.2 mg (62%). Found: C 30.6, H 3.66, N 2.95. C₂₂H₂₆N₂F₆O₈RuS₆·(CH₃)₂SO (932.00) requires: C 30.9, H 3.46, N 3.00%.

δ_{H} (D₂O): 2.43 (s, 3 H, CH₃), 2.50–3.90 (m, 16 H, CH₂ [12]aneS4), 7.38 (d, 1 H, H5'), 7.79 (d, 1 H, H5), 8.28 (s, 1 H, H3'), 8.61 (s, 1 H, H3), 9.05 (br m, H6'), 9.34 (br m, 1 H, H6). δ_{H} (acetone-*d*₆): 2.68 (s, 3 H, CH₃), 2.50–4.30 (m, 16 H, CH₂ [12]aneS4), 7.71 (d, 1 H, H5'), 8.15 (d, 1 H, H5), 8.96 (s, 1 H, H3'), 9.10 (s, 1 H, H3), 9.43 (br m, 1 H, H6'), 9.81 (br m, 1 H, H6).

[Bpy₄-PP{Ru([12]aneS4)}₄][NO₃]₈ (13). To a 20.0 mg amount of bpy₄-PP (0.014 mmol) dissolved in 10 mL of CHCl₃ a solution of [Ru([12]aneS4)(dmsO-S)(NO₃)]NO₃ (31.7 mg, 0.058 mmol) dissolved in 45 mL of methanol was added. The resulting solution was heated to reflux for 8 h (the reaction was monitored by TLC, silica plates, CHCl₃-EtOH 9 : 1). The solution was concentrated under vacuum to *ca.* 15 mL. Dropwise addition of diethyl ether (*ca.* 2 mL) induced the formation of a precipitate, that was removed by filtration, washed with diethyl ether and dried under vacuum. Yield: 32 mg (69%).

δ_{H} (CD₃NO₂): -2.72 (br s, 2 H, NH), 2.72 (s, 12 H CH₃), 2.80–3.90 (m, CH₂ [12]aneS4), 7.64 (d, 4 H, *J* = 5.2 Hz, H5'), 8.40 (m, 20 H, H5 + *mbg* + *obg*), 8.87 (s, 4 H, H3'), 9.09 (br, 8 H, β H), 9.30 (br m, 4 H, H6'), 9.43 (s, 4 H, H3), 9.69 (br m, 4 H, H6), 10.92 (br s, 4 H, CONH). δ_{H} (CD₃NO₂, *T* = -15 °C): -2.81 (br s, 2 H, NH), 2.68 (s, 12 H CH₃), 2.80–3.90 (m, CH₂ [12]aneS4), 7.61 (d, 4 H, *J* = 4.6 Hz, H5'), 8.41 (m, 20 H, H5 + *mbg* + *obg*), 8.85 (s, 4 H, H3'), 9.10 (br, 8 H, β H), 9.37 (d, 4 H, H6'), 9.44 (s, 4 H, H3), 9.75 (d, 4 H, H6), 11.13 (br s, 4 H, CONH). UV-vis λ_{max} (CH₃NO₂)/nm (relative intensity (%)): 423 (100), 517 (5.8), 554 (4.9), 592 (2.6), 649 (2.6).

[Bpy₄-PP{Ru([12]aneS4)}₄][Cl]₈ (14). To a 20.0 mg amount of bpy₄-PP (0.014 mmol) dissolved in 10 mL of CHCl₃ a solution of [Ru([12]aneS4)(dmsO-S)Cl][Cl] (28.6 mg, 0.058 mmol) dissolved in 45 mL of methanol was added. The resulting solution was heated to reflux for 15 h (the reaction was monitored by TLC, silica plates, CHCl₃-EtOH 9 : 1), during which time a fine purple precipitate formed. The solid was removed by filtration and washed with diethyl ether and dried under vacuum. The mother liquor was concentrated under vacuum to *ca.* 15 mL. Dropwise addition of diethyl ether (*ca.* 10 mL) induced the formation of a second batch of precipitate, that was treated as above. Total yield: 30 mg (70%).

δ_{H} (DMSO-*d*₆): -2.83 (br s, 2 H, NH), 2.67 (s, 12 H CH₃), 2.70–4.10 (m, CH₂ [12]aneS4), 7.39 (m, 4 H, H5'), 8.09 (m, 4 H, H5), 8.32 (m, 20 H, H3' + *mbg* + *obg*), 8.67 (m, 4 H, H6'), 8.98 (m, 16 H, β H + H6' + H3), 11.14 (br s, 4 H, CONH). UV-vis λ_{max} (DMSO)/nm (relative intensity (%)): 426 (100), 519 (4.5), 557 (3.7), 594 (1.7), 651 (1.9).

Crystallographic data

Crystals of **4** and **10** suitable for X-ray diffraction were obtained by layering diethyl ether on top of nitromethane solutions of the products.

Data collection for **4** was performed at the X-ray synchrotron Elettra diffraction beamline, Trieste (Italy), using a monochromatized wavelength of 1.00 Å at 100 K, whereas that for **10** was carried out on a Nonius DIP-1030H system (MoK α radiation, λ = 0.71073 Å, graphite monochromatized, room temperature). Cell refinement, indexing and scaling of the data sets were performed using programs Denzo and Scalepack.⁴⁵ Both structures were solved by direct methods and subsequent Fourier analyses,⁴⁶ and refined by the full-matrix least-squares method based on *F*² with all observed reflections.⁴⁶ In **4** some restraints on bond distances were applied to the disordered eight CF₃SO₃⁻ anions, which affect the crystal quality. Moreover, 13.5% of the unit cell is solvent accessible void and the Δ Fourier map revealed the presence of two nitromethane molecules in the asymmetric unit. The contribution of hydrogen atoms at calculated positions were included in final cycles of refinement. All the calculations were performed using the WinGX System, Ver 1.80.05.⁴⁷

Crystal data and details of data collections and refinements for the structures are summarized in Table 1. A selection of coordination bond lengths (Å) and angles (°) for **4** is reported in Table 2.

Table 1 Crystallographic data and details of structure refinements for compounds **4** and **10**

	4 (CH ₃ NO ₂)	10
Empirical formula	C ₁₁₆ H ₁₁₈ F ₂₄ N ₂₀ O ₃₂ Ru ₄ S ₂₀	C ₂₂ H ₂₈ F ₆ N ₂ O ₉ RuS ₆
Formula weight	3805.78	871.89
Crystal system	Monoclinic	Monoclinic
Space group	<i>P</i> ₂ / <i>c</i>	<i>P</i> ₂ / <i>c</i>
<i>a</i> /Å	23.157(5)	10.026(3)
<i>b</i> /Å	16.581(4)	23.075(4)
<i>c</i> /Å	20.833(5)	14.057(3)
β /°	97.01(3)	96.40(2)
<i>V</i> /Å ³	7939(3)	3231.8(13)
<i>Z</i>	2	4
<i>D</i> _{calcd} /g cm ⁻³	1.592	1.792
μ /mm ⁻¹	0.890	0.958
<i>F</i> (000)	3844	1760
θ _{max} /°	25.52	28.28
Reflections collected	49 860	35 958
Unique reflections	4833	7081
<i>R</i> _{int}	0.0404	0.0532
Observed <i>I</i> > 2σ(<i>I</i>)	3965	4120
Parameters	733	418
GOF	1.117	0.870
<i>R</i> 1 (<i>I</i> > 2σ(<i>I</i>)) ^a	0.0844	0.0427
<i>wR</i> ₂ ^a	0.2515	0.1043
$\Delta\rho/e$ Å ⁻³	1.161 ^b –0.831	0.420–0.425

^a $R_1 = \sum \|F_o\| - |F_c| / \sum |F_o|$, $wR_2 = [\sum w(F_o^2 - F_c^2)^2 / \sum w(F_o^2)]^{1/2}$.^b Residual peak close to a triflate anion.**Table 2** Selected coordination bond lengths (Å) and angles (°) for compound **4**

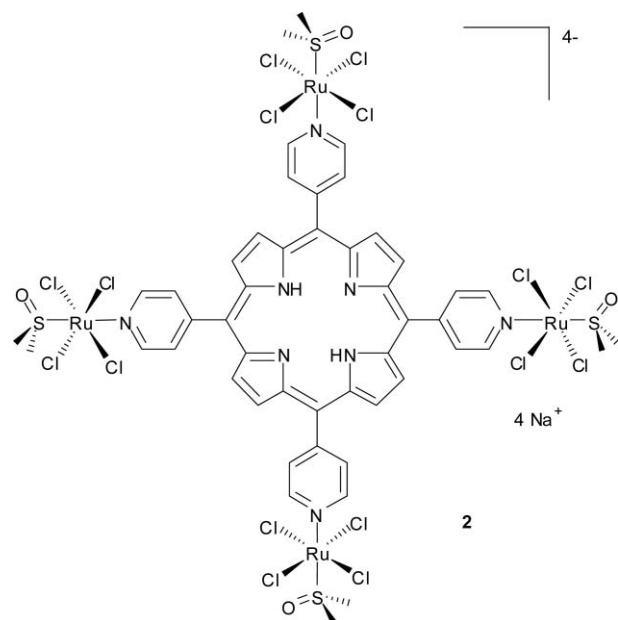
Bond lengths/Å			
Ru(1)–N(1)	2.175(12)	Ru(2)–N(3)	2.152(12)
Ru(1)–N(2)	2.165(12)	Ru(2)–N(4)	2.163(12)
Ru(1)–N(5)	2.194(11)	Ru(2)–N(6)	2.212(12)
Ru(1)–S(1)	2.376(4)	Ru(2)–S(4)	2.381(5)
Ru(1)–S(2)	2.378(5)	Ru(2)–S(5)	2.361(4)
Ru(1)–S(3)	2.376(4)	Ru(2)–S(6)	2.365(5)
Bond angles/°			
N(1)–Ru(1)–N(2)	76.6(5)	N(3)–Ru(2)–N(4)	78.4(5)
N(1)–Ru(1)–N(5)	87.4(4)	N(3)–Ru(2)–N(6)	88.2(4)
N(1)–Ru(1)–S(1)	175.6(4)	N(3)–Ru(2)–S(4)	96.8(4)
N(1)–Ru(1)–S(2)	96.6(4)	N(3)–Ru(2)–S(5)	175.7(4)
N(1)–Ru(1)–S(3)	92.7(3)	N(3)–Ru(2)–S(6)	91.7(3)
N(2)–Ru(1)–N(5)	84.5(4)	N(4)–Ru(2)–N(6)	87.0(5)
N(2)–Ru(1)–S(1)	99.1(4)	N(4)–Ru(2)–S(4)	174.9(4)
N(2)–Ru(1)–S(2)	172.2(4)	N(4)–Ru(2)–S(5)	97.4(4)
N(2)–Ru(1)–S(3)	95.3(3)	N(4)–Ru(2)–S(6)	94.0(4)
N(5)–Ru(1)–S(1)	91.6(3)	N(6)–Ru(2)–S(4)	91.1(3)
N(5)–Ru(1)–S(2)	91.4(3)	N(6)–Ru(2)–S(5)	91.0(3)
N(5)–Ru(1)–S(3)	179.8(4)	N(6)–Ru(2)–S(6)	179.0(4)
S(1)–Ru(1)–S(2)	87.70(16)	S(4)–Ru(2)–S(5)	87.43(16)
S(1)–Ru(1)–S(3)	88.32(15)	S(4)–Ru(2)–S(6)	87.91(17)
S(2)–Ru(1)–S(3)	88.83(16)	S(5)–Ru(2)–S(6)	89.12(16)

Results

Conjugates through single-bond coordination

Conjugates with *meso* 4'-tetrapyrrolylporphyrin (4'-TPyP). We reported that treatment of 4'TPyP with the Ru(III) precursor [*n*-Bu₄N][*trans*-RuCl₄(dms_o-S)₂] affords the tetra-anionic Ru(III)-conjugate [*n*-Bu₄N]₄[4'TPyP{*trans*-RuCl₄(dms_o-S)₄] (**1**).⁴⁸ This

porphyrin bears four NAMI-type fragments (with a *meso* pyridyl group instead of imidazole as axial N-donor ligand *trans* to dms_o-S, Fig. 1) and is therefore of interest for its potential antimetastatic properties.¹¹ However compound **1**, being totally insoluble in aqueous solution, is as such unsuited for biological tests. We found that the corresponding sodium salt, [Na]₄[4'TPyP{*trans*-RuCl₄(dms_o-S)₄] (**2**, Fig. 2) can be obtained in almost quantitative yield by treatment of **1** with excess Na[B(C₆H₅)₄] in nitromethane solution.

**Fig. 2** Schematic structure of [Na]₄[4'TPyP{*trans*-RuCl₄(dms_o-S)₄] (**2**).

Compound **2** is well soluble in aqueous solution, where it shows the typical broad NMR resonance for dms_o-S bound to a Ru(III) paramagnetic center at *ca.* $\delta = -13$.^{11,48} Similar to the corresponding model complex Na[*trans*-RuCl₄(dms_o-S)(py)] (and to NAMI-A), the stability of compound **2** in aqueous solution—as evaluated from the changes of its electronic absorption spectrum in the visible range—depends strongly on pH. The compound is essentially stable at mildly acidic pH (25.0 °C), whereas a *ca.* four-fold decrease of intensity of the Soret band, accompanied by remarkable broadening, was observed within 3 h at pH 7.4 (ESI).[†] At this pH stepwise dissociation of chlorides from the Ru(III) fragments is expected to occur.¹¹ Since it is unlikely that chloride dissociation from the peripheral Ru centers affects significantly the electronic absorption spectrum of the porphyrin, the observed spectral changes were attributed to aggregation as a consequence of the progressive decrease of the negative charge of **2**. The general increase of the background absorption in the whole visible range registered for longer observation times suggests that, as found for the NAMI-type Ru(III) complexes,¹¹ formation of polynuclear aggregates with μ -oxo or μ -hydroxo bridges between Ru(III) centers occurs.

We also performed the coordination of 4'TPyP to half-sandwich Ru(II) fragments. We have recently investigated the cytotoxicity of Ru(II)-[9]aneS3 complexes ([9]aneS3 = 1,4,7-trithiacyclononane) of the type [Ru([9]aneS3)(N-N)Cl][CF₃SO₃], [Ru([9]aneS3)(N-N)(dms_o-S)][CF₃SO₃]₂ (N-N = nitrogen chelating ligand such

as ethane-1,2-diamine (en), bpy, or substituted bpy), and [Ru([9]aneS3)(η^2 -dicarb)(dmsO-S)] (dicarb = oxalate, malonate, methylmalonate).^{39,49} These complexes are structurally similar to antitumour active organometallic half-sandwich compounds,¹³ with the face-capping sulfur macrocycle replacing the aromatic fragment.

We report now that treatment of 4'TPyP with a slight excess of [Ru([9]aneS3)(en)Cl][CF₃SO₃] (in the presence of Ag(CF₃SO₃) for removing the chlorido ligand) affords the octacationic conjugate [4'TPyP{Ru([9]aneS3)(en)}₄][CF₃SO₃]₈ (**3**) in excellent yield. Compound **3**, beside being soluble in organic solvents such as methanol and nitromethane, is also well soluble in aqueous solution. Overall, the ¹H NMR spectrum of **3** is consistent with the symmetry of the compound: all peripheral Ru fragments are equivalent. All proton resonances are sharp at 20 °C, with the exception of the β H signal that is remarkably broad (see below). The four equivalent pyridyl rings give two well resolved doublets in the aromatic region of the spectrum. The upfield region is similar to that of the precursor Ru complex: in D₂O the two pairs of diastereotopic protons on the equivalent NH₂ groups give two well resolved resonances at δ = 4.17 and 5.09 (coupled in the H–H COSY spectrum), whereas the CH₂ protons of en and of [9]aneS3 resonate as a series of partially overlapping multiplets between δ = 2.6 and 3.1 (ESI).[†] Only four aliphatic ¹³C resonances are observed in the HSQC spectrum (one for the en carbons and three for the [9]aneS3 carbons), consistent with a C_s symmetry in solution for each equivalent Ru fragment, as found in the precursor.³⁸

The corresponding conjugate with bpy in the place of en, [4'TPyP{Ru([9]aneS3)(bpy)}₄][CF₃SO₃]₈ (**4**), was obtained by treatment of 4'TPyP with [Ru([9]aneS3)(bpy)(dmsO-S)][CF₃SO₃]₂ upon replacement of dmsO by the pyridyl groups. Compound **4** was also characterized in the solid state by X-ray crystallography: the tetranuclear cation is composed of four [Ru([9]aneS3)(bpy)]²⁺ units bound to the *meso* pyridyl moieties in a centro-symmetric arrangement (Fig. 3).

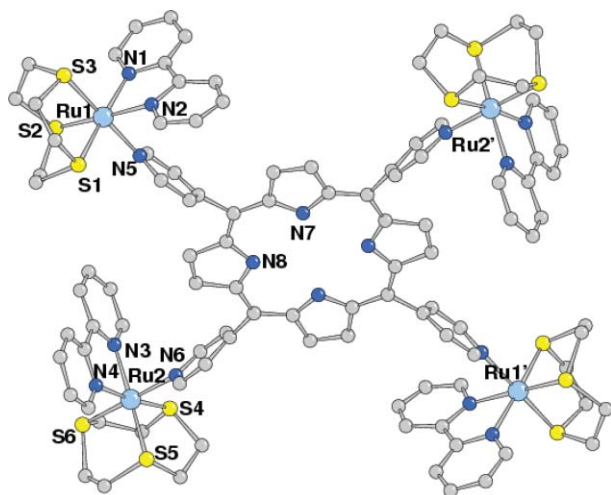


Fig. 3 Molecular structure of the centro-symmetric complex cation of [4'TPyP{Ru([9]aneS3)(bpy)}₄][CF₃SO₃]₈ (**4**).

The cation presents a pseudo four fold axis normal to the porphyrin mean plane: the four Ru fragments are iso-oriented, with intermetallic side distances of 14.303(4) Å (Ru1 \cdots Ru2) and

14.213(3) Å (Ru1 \cdots Ru2'). The Ru centers have a distorted octahedral coordination sphere, with Ru–S and Ru–N(bpy) coordination distances that average to 2.17(1) Å and 2.373(5) Å, respectively, (*i.e.* they are longer by *ca.* 0.05 and 0.03 Å, respectively, than those found in the Ru(II) precursor).³⁸ The two independent *meso* pyridyl rings N5 and N6 form a dihedral angle with the porphyrin mean plane of *ca.* 68° and deviate slightly from a linear coordination, with Ru–N(py) \cdots C(*meso*) angles significantly narrower than 180° (168.3 and 172.9°, respectively). As a consequence, the bpy ligands are considerably canted towards the adjacent *meso* pyridyl rings (dihedral angles between the mean planes of 62.4(4) and 72.8(4)°, Fig. 4). A pyridine ring of each bpy is located approximately in the porphyrin plane (Fig. 4), at a distance of *ca.* 4.45 Å from a pyrrole hydrogen atom. This feature, probably dictated by packing effects, might be compatible with weak CH \cdots π interactions.

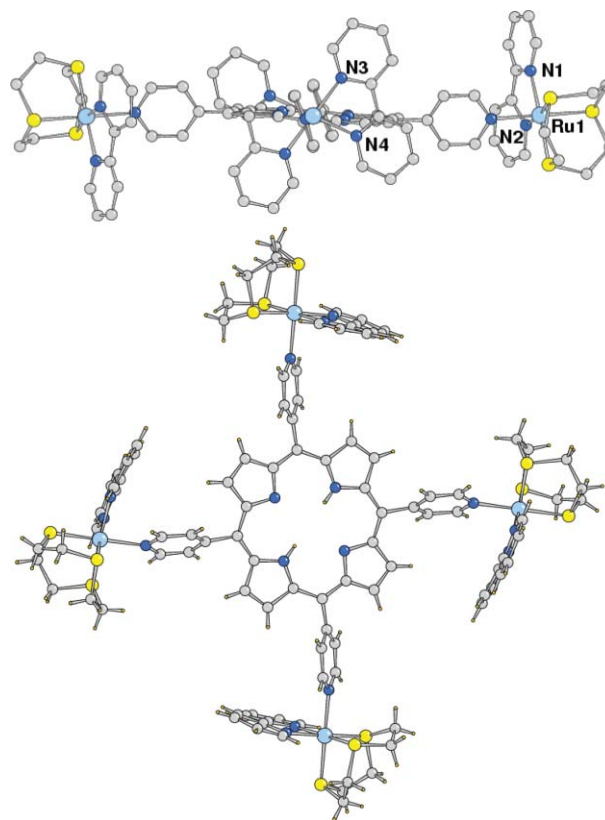


Fig. 4 Top: side view of the complex cation of **4** along the Ru2 \cdots Ru2' direction ([9]aneS3 ligands at Ru2 ions omitted for clarity). Bottom: top view showing the canting of the bpy ligands towards the pyrrole rings.

Compound **4** is mildly soluble in water, but becomes soluble upon addition of 0.02% of DMSO and also in phosphate buffer at pH 7.4. As for **3**, the ¹H NMR spectrum of **4** in CD₃OD shows sharp signals at 20 °C (with the exception of the β H resonance, see below) and is consistent with the symmetry of the molecule (ESI).[†] The single set of bpy and pyridyl signals (four and two, respectively) implies that all four metal fragments are equivalent and that each of them has a C_s symmetry. The anisotropic shielding of the bpy rings, that are perpendicular to the plane of the porphyrin, more than counteracts the deshielding typically observed upon coordination of 4'TPyPs to Ru(II) fragments;⁴⁸ as a consequence, the resonances of 4'TPyP are shifted slightly upfield

compared to **3** (δ H2,6 = 9.12 in **4** vs. 9.31 in **3**; δ H3,5 = 8.11 in **4** vs. 8.41 in **3**).

As already mentioned, both **3** and **4** have very broad β H resonances at 20 °C, suggesting the occurrence of conformational equilibria. Variable-temperature (VT) NMR experiments showed that for **3**, in CD₃NO₂ solution, the resonance of the eight pyrrole protons becomes a sharp singlet at 65 °C, whereas at -30 °C in CD₃OD solution it splits into two equally intense sharp singlets (δ = 9.30 and 8.97, ESI)† that are not correlated in the H-H COSY spectrum but show a strong exchange crosspeak in the ROESY spectrum. The β H resonance of the bpy derivative **4** has a very similar temperature dependence in CD₃OD-CD₃NO₂ (99 : 1) solution and splits into two equally intense sharp singlets at -40 °C (δ = 8.89 and 8.51, ESI).† The upfield singlet was assigned to the four pyrrole protons that are directly shielded by the bpy rings. The β H NMR pattern found for both **3** and **4** at low *T* is compatible with the presence in solution of a frozen conformer with a *D*_{2h} symmetry, with adjacent Ru fragments arranged in a pairwise fashion: en (or bpy) ligands on Ru units at *meso* positions 5, 10 (and 15, 20) face each other, while those on the *meso* positions 5, 20 (and 10, 15) are far apart (Fig. 5). The two types of β H protons, a and b, are exchanged by the concerted rotation of the four Ru complexes. This geometry is different from that found in the solid state for **4**, where all Ru fragments are iso-oriented, but is similar to that found by us for the Re(I) conjugate [4'TPyP{Re(CO)₃(bpy)}₄][CF₃SO₃]₄.⁵⁰

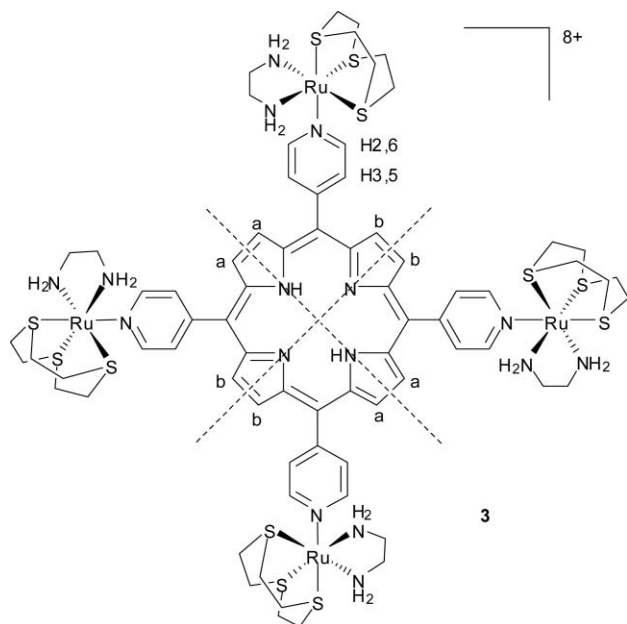


Fig. 5 Schematic structure of the prevailing conformer of **3** at low *T*. Dotted lines indicate the two symmetry planes. The two sets of β H protons, responsible for the two singlets in the low *T* NMR spectrum, are labelled a and b.

Both porphyrin conjugates **3** and **4** are very stable in aqueous solution and in phosphate buffer at physiological pH: their NMR and visible spectra remain unchanged for hours. This behaviour is consistent with the substitutionally inert coordination sphere of the Ru(II) fragments.

Conjugates with 4'-monopyridylporphyrins. Conjugates of 4'-monopyridylporphyrin (4'-MPyP), with a single peripheral Ru fragment, are typically not water soluble, regardless of the charge of the complex. However, they may become soluble if the three *meso* phenyl rings are functionalized with appropriate groups. Along this strategy, that was used already for Pt and Ru-polypyridyl conjugates,^{8,32} we prepared the series of *meso*-pyridyl/carboxyphenyl porphyrins with the aim of exploiting the pyridyl N atoms for coordination to Ru fragments and the deprotonation of the carboxylic groups at physiological pH for increasing water solubility.⁴² We report here the monoruthenated adduct Na[*trans*-RuCl₄(dmsos)(4'-MPyCbPP)] (**5**, Fig. 6), where 4'-MPyCbPP = 5-(4'-pyridyl)-10,15,20-tris(4'-carboxyphenyl)porphyrin, in which the coordination sphere of Ru(III) is again very similar to that of NAMI. Compound **5**, that was conveniently obtained by cation exchange from the corresponding tetrabutylammonium salt, is sparingly soluble in water, but becomes soluble in phosphate buffer solution at pH 7.4. At this pH, time-dependent spectral changes similar to those of compound **2**, but less pronounced (suggesting the occurrence of less aggregation), were observed.

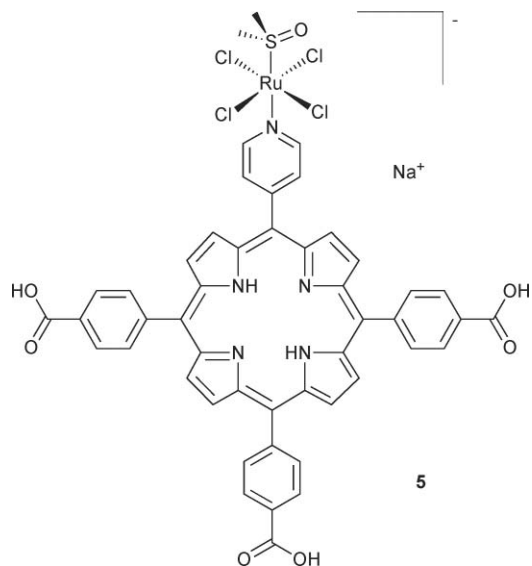


Fig. 6 Schematic drawing of Na[*trans*-RuCl₄(dmsos)(4'-MPyCbPP)] (**5**).

Conjugates through two-bond coordination

We report here the preparation and characterization of a series of porphyrins that bear from 1 to 4 peripheral bpy moieties at *meso* positions, *meso*-(*p*-bpy-phenyl)porphyrins (bpy_{*n*}-PPs, *n* = 1–4) (Fig. 7) and their conjugates with half-sandwich Ru(II) fragments. Bpy_{*n*}-PPs were obtained by coupling of *meso*-(*p*-aminophenyl)porphyrins, *p*(NH₂)_{*n*}PPs (*n* = 1–4), with 4-methyl-2,2'-bipyridine-4'-carboxylic acid (bpyAc).

Re(I) conjugates of Zn·Bpy-PP have been extensively investigated for their photophysical properties by Perutz and co-workers.⁵¹ A heteroleptic Re(I)/Ru(II) conjugate of Zn·Bpy₂-*cis*PP has been also described.⁵²

Details for the stepwise preparation of bpy_{*n*}-PPs are reported in the experimental section. Bpy₃-PP and bpy₄-PP are described

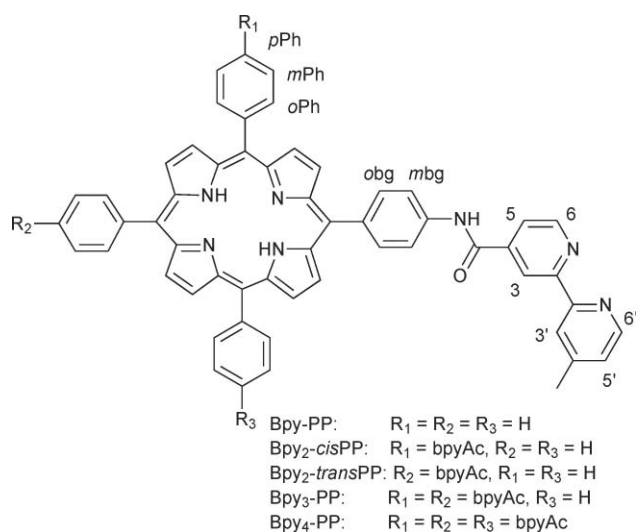


Fig. 7 Schematic drawing of bpy_n-PPs, *n* = 1–4.

here for the first time. The ¹H NMR spectra of bpy_n-PPs in CDCl₃ solution are quite similar to one another (with the obvious exception of the relative intensities of the bpyAc and of the phenyl resonances that depend on *n*). Assignments, performed through conventional 2D correlation spectra, were consistent with those already reported in the literature for bpy-PP and bpy₂-*cis*PP.^{51,52} The spectrum of bpy-PP is reported in Fig. 8 as a representative example.

For each porphyrin the six inequivalent bpyAc protons give six resolved resonances (four doublets and two singlets). The most downfield of them is typically the H6 doublet, often partially overlapped with the βH resonance. The chemical shifts of all the aromatic resonances, and that of H3 in particular, were found to depend on the concentration probably because of aggregation mediated by π–π stacking.[§] The singlet of the methyl group in 4' position, that falls at *ca.* δ = 2.5, is correlated in a NOESY spectrum to the resonances of the adjacent H3' and H5' protons. This feature, in conjunction with the H–H COSY spectrum, allowed us to distinguish the two inequivalent halves of bpyAc. The amidic NH resonance typically falls in the range

§ Depending on the solvent and concentration, in some cases the H3 singlet can resonate more upfield than the H6' doublet.

δ = 10–11 and rapidly decreases in time due to H/D exchange with the solvent. The two isomeric disubstituted porphyrins, bpy₂-*cis*PP and bpy₂-*trans*PP, can be unambiguously distinguished only by a close examination of the resonances of the pyrrole protons: two doublets of 4 H each for the *trans* isomer and two (partially overlapped) singlets and two doublets of 2 H each for the *cis* isomer (ESI).^{†48} As expected, the spectrum of bpy₄-PP is the simplest of the series and the eight equivalent pyrrole protons resonate as a singlet.

With the exception of bpy₂-*trans*PP, whose amount was insufficient, all bpy_n-PPs were treated with an appropriate amount of the half-sandwich Ru(II) precursor [Ru([9]aneS3)(dmsO)₃][CF₃SO₃]₂ in CHCl₃–CH₃NO₂ or CHCl₃–acetone mixtures: replacement of two adjacent dmsO ligands by the bpy moieties afforded the corresponding conjugates [bpy_n-PP{Ru([9]aneS3)(dmsO-S)}_n][CF₃SO₃]_{2n} (**6**, *n* = 1; **7**, *n* = 2; **8**, *n* = 3; **9**, *n* = 4; ESI)[†] in acceptable-to-good yields. All conjugates (Fig. 9) have been characterized by mono- and bidimensional NMR spectroscopy (they are soluble in CDCl₃, CD₂Cl₂, CD₃NO₂, DMSO but scarcely soluble in water) and give consistent molecular peaks in ESI-MS mass spectra (in each case the molecular peak corresponds to the conjugate in which each dmsO-S ligand has been replaced by a triflate anion).

The previously reported model complex [Ru([9]aneS3)(bpyAc)(dmsO-S)][CF₃SO₃]₂ (**10**)³⁹ was now characterized also by X-ray crystallography (Fig. 10) and used as reference for NMR assignments.

In general, all proton NMR resonances of conjugates **6–9** are slightly broader than those in the free porphyrin or in the model complex **10**. The ¹H NMR spectrum of [bpy₃-PP{Ru([9]aneS3)(dmsO-S)}₃][CF₃SO₃]₆ (**8**) is described in detail as an example (Fig. 11).

The upfield region, beside the multiplets of [9]aneS3 (δ = 2.5–3.4), shows three singlets of equal intensities between δ 2.7 and 2.9. By analogy with the spectrum of **10**, the upfield singlet was attributed to the methyl on bpyAc (attribution confirmed by the NOESY experiment) and the other two to the diastereotopic methyls of dmsO-S.[¶] In the downfield region, the

¶ As in the ¹H NMR spectrum of **10**, the dmsO-S resonances are shifted upfield compared to their usual range by the anisotropic shielding of the adjacent bpy moiety.

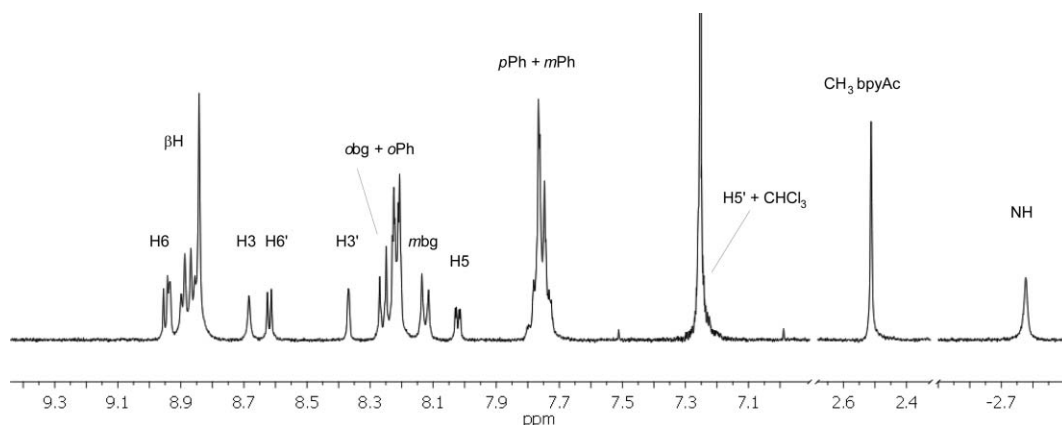


Fig. 8 ¹H NMR spectrum (500 MHz) of bpy-PP in CDCl₃. See Fig. 7 for labelling scheme.

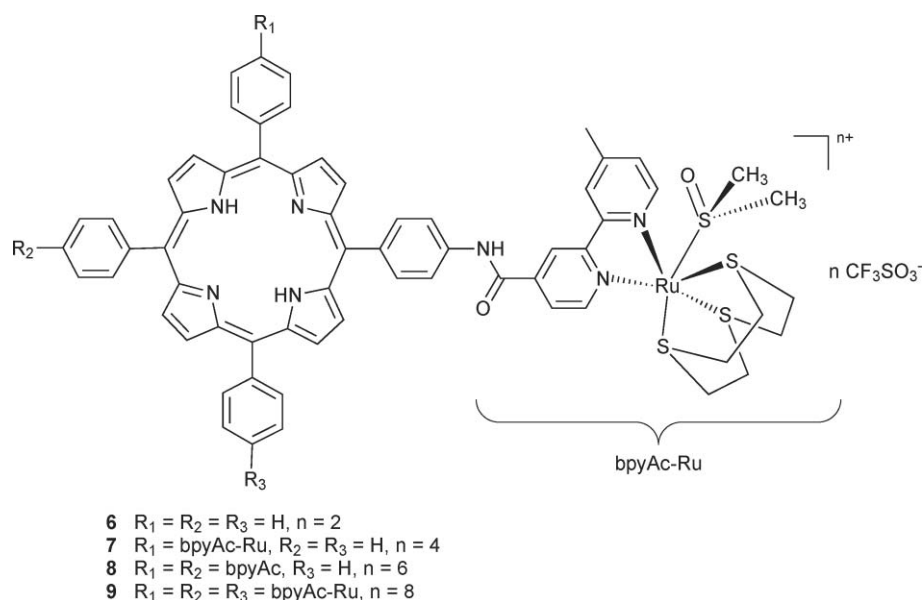


Fig. 9 Schematic drawing of conjugates $[\text{bpy}_n\text{-PP}\{\text{Ru}(\text{[9]aneS3})(\text{dmsO-S})\}_n][\text{CF}_3\text{SO}_3]_{2n}$ (6–9).

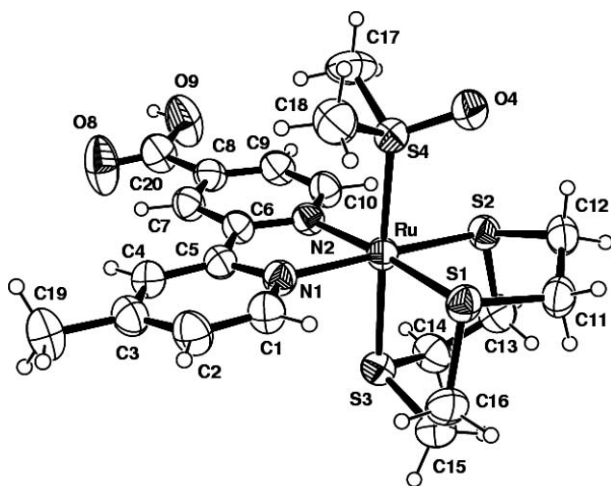


Fig. 10 ORTEP drawing (40% probability ellipsoid) of the complex cation of **10**.

six resonances of the bpyAc protons maintain the same order as in the free bpy-PP. The resonances of H5,5' are scarcely affected by coordination to Ru, whereas those of H6,6' and H3,3' are shifted downfield by *ca.* 0.2 ppm. As in the free porphyrin, in **8** the resonances of the moiety at *meso* position 10 could not be distinguished from those at the equivalent *meso* positions 5 and 15. The symmetry of this T-shaped compound was reflected only in the resonances of the amidic NH protons that in CD_3NO_2 give two well resolved singlets of 2 : 1 intensity ratio at $\delta = 9.92$ (the two equivalent NHs at *meso* positions 5,15) and $\delta = 9.99$ (NH at *meso* position 10) (Fig. 11). In the more symmetrical $[\text{bpy}_2\text{-cisPP}\{\text{Ru}(\text{[9]aneS3})(\text{dmsO-S})\}_2][\text{CF}_3\text{SO}_3]_4$ (**7**) and $[\text{bpy}_4\text{-PP}\{\text{Ru}(\text{[9]aneS3})(\text{dmsO-S})\}_4][\text{CF}_3\text{SO}_3]_8$ (**9**) conjugates, the peripheral Ru fragments are equivalent. The resonance of the pyrrole protons, that in **6** is moderately broad at 20 °C, becomes broader upon increasing the number of peripheral Ru compounds (Fig. 11).

As evidenced by ^1H NMR spectroscopy, in aqueous solution the reference compound **10** slowly releases the dmsO-S; according to integration, at equilibrium (after *ca.* 5 d at 25 °C) almost equal amounts of **10** and of its aquated derivative $[\text{Ru}(\text{[9]aneS3})(\text{bpyAc})(\text{H}_2\text{O})]^{2+}$ were found (ESI).[†] Despite being scarcely soluble in water, conjugates **7–9** become moderately soluble in 50 mM phosphate buffer at pH 7.4 (the solubility increases upon increasing the charge). At 25.0 °C the visible spectrum of each conjugate in this medium remains basically unchanged in shape for hours, except for a slow progressive decrease of intensity (*ca.* 2.5% in 1 h) that might be compatible with the replacement of dmsO with water in the peripheral Ru moieties, a process that—by itself—is not expected to affect significantly the electronic absorption spectrum of the porphyrin chromophore. The stability of the spectra also suggests that no significant aggregation occurs in solution.

Optically matched DMSO solutions of $\text{bpy}_4\text{-PP}$ and conjugate **9** showed very similar fluorescence spectra upon selective excitation at the Soret band ($\lambda_{\text{exc}} = 425$ nm, $\lambda_{\text{em}} = 656$ nm). The emission intensity of **9** is *ca.* 20% lower than that of the parent porphyrin (ESI),[†] as expected because of the peripheral heavy atoms.²⁰

Finally, the tetra-ruthenated porphyrin conjugate $[\text{bpy}_4\text{-PP}\{\text{Ru}(\text{[12]aneS4})_4][\text{CF}_3\text{SO}_3]_8$ (**11**, Fig. 12), in which the peripheral Ru fragments have no labile ligands, was prepared in good yield by reaction of $\text{bpy}_4\text{-PP}$ with a slight excess of the Ru(II) precursors $[\text{Ru}(\text{[12]aneS4})(\text{dmsO-S})(\text{H}_2\text{O})][\text{CF}_3\text{SO}_3]_2$ ([12]aneS4 = 1,4,7,10-tetrathiacyclododecane).⁴¹

We also prepared the corresponding model complex $[\text{Ru}(\text{[12]aneS4})(\text{bpyAc})][\text{CF}_3\text{SO}_3]_2$ (**12**) as a reference for NMR purposes. The downfield region of the ^1H NMR spectrum of **11** in deuterated acetone or nitromethane is similar to that of **9**, with the additional feature that, beside the βH resonance, also the doublets of H6 and H6' are quite broad at 20 °C (Fig. 13). The same broadening of the signals of H6 and H6' was observed in the spectrum of the model complex **12** (ESI),[†] and of the corresponding bpy complex as well, and it was attributed to

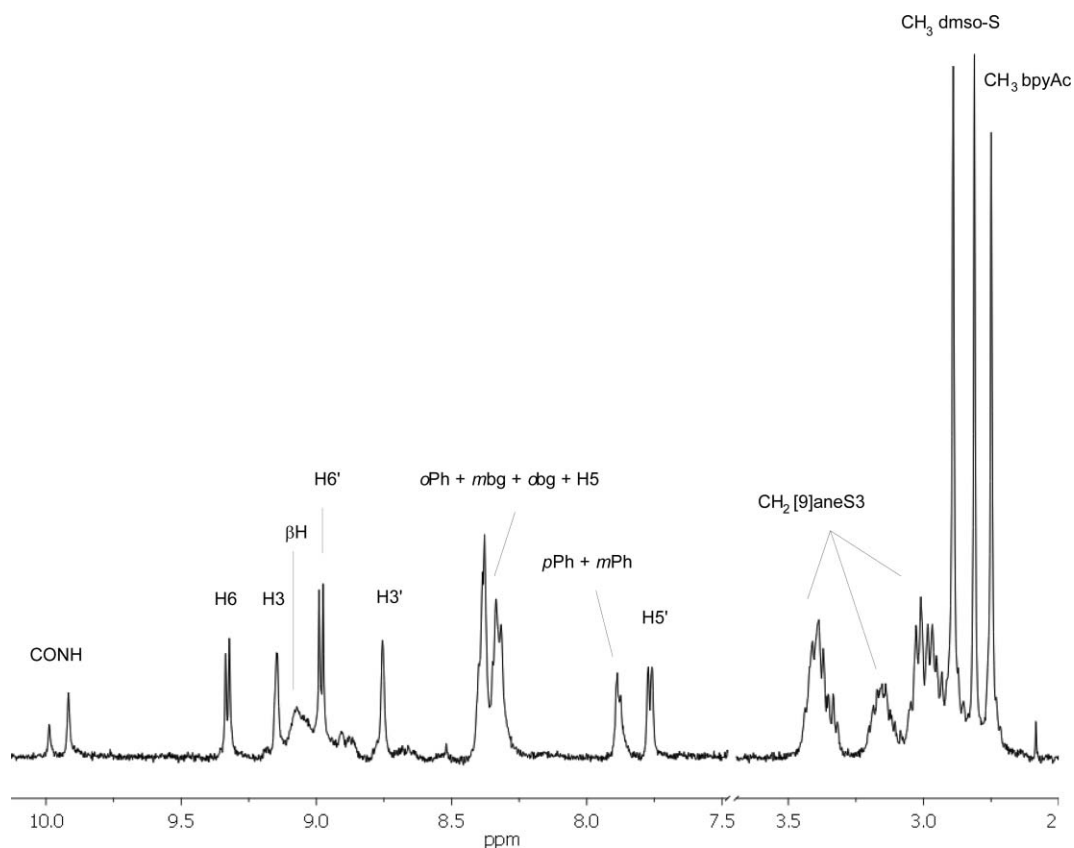


Fig. 11 ^1H NMR spectrum (500 MHz, 20 °C) of $[\text{bpy}_3\text{-PP}\{\text{Ru}(\text{9)aneS3}(\text{dmsO-S})\}_3][\text{CF}_3\text{SO}_3]_6$ (**8**) in CD_3NO_2 . See Fig. 7 for labelling scheme.

conformational equilibria of the [12]aneS4 ligand.⁵³ The H6 and H6' resonances became two sharp doublets upon lowering the temperature to -40 °C (acetone- d_6), whereas at -60 °C the βH resonance split into two equally intense sharp singlets (Fig. 13). This last feature is similar to what already observed for **3** and **4** and might be attributed to the presence, at low T , of a prevailing conformer in which the four lateral *meso* arms are oriented in pairwise fashion (see above).

With the aim of assessing how the solubility of this 8+ tetra-ruthenated porphyrin conjugate is affected by the nature of the counter anion, also the corresponding nitrate and chloride compounds $[\text{bpy}_4\text{-PP}\{\text{Ru}(\text{12)aneS4}\}_4][\text{NO}_3]_8$ (**13**) and $[\text{bpy}_4\text{-PP}\{\text{Ru}(\text{12)aneS4}\}_4][\text{Cl}]_8$ (**14**) (Fig. 12) were prepared by reaction of $\text{bpy}_4\text{-PP}$ with the Ru(II) precursors $[\text{Ru}(\text{12)aneS4}(\text{dmsO-S})\text{X}][\text{X}]$ ($\text{X} = \text{Cl}, \text{NO}_3$, respectively). The ^1H NMR spectra of **13** and **14** are very similar to that of **11**. No significant difference in the solubility in aqueous solution was observed: the three conjugates **11**, **13** and **14** are sparingly soluble in water and become moderately soluble in phosphate buffered solution at physiological pH.

Discussion

The motivation for making water-soluble porphyrin conjugates with Ru fragments that are structurally similar to anticancer compounds are quite obvious and were detailed in the Introduction already. The NAMI-type conjugates with *meso*-tetrapyrrolylporphyrin and with *meso*-pyridyl/carboxyphenyl porphyrins described in this work, as well as the conjugates of bpy_n -

PPs with half-sandwich Ru(II) compounds, will be preliminary tested *in vitro* for anticancer activity, both in the dark and under illumination in the porphyrin absorption region. They are either soluble in water or DMSO. Those conjugates that are not well soluble in aqueous solution, usually become moderately soluble in phosphate buffer at physiological pH.

For potential PDT applications it is important that the porphyrin conjugates have a low general toxicity (high IC_{50}) and become cytotoxic only in selected locations upon activation with visible light.^{15,32,34} Our cationic Ru compounds are scarcely cytotoxic in the dark, thus they seem to be appropriate candidates for conjugation to porphyrins with the aim of obtaining photocytotoxicity.

It is perhaps less obvious why it might be worth preparing and investigating in the biomedical context porphyrin conjugates with coordinatively saturated Ru fragments. We have recently reported that a number of coordinatively saturated and substitutionally inert metal complexes, including Ru, that we defined as *structural compounds*, have indeed interesting biological properties (*e.g.* as enzyme inhibitors, DNA intercalators).¹⁹ Coordination of such compounds to porphyrins might result in novel attractive features.

In general, peripherally bound inert Ru compounds, beside improving water solubility (if appropriately chosen) are expected to alter the redox and photophysical parameters of the porphyrin, and to influence significantly its biodistribution. The metal fragments will also affect the steric profile of the porphyrin and might introduce additional functionalities. In particular, the total charge of the porphyrin–Ru conjugates can be tuned according

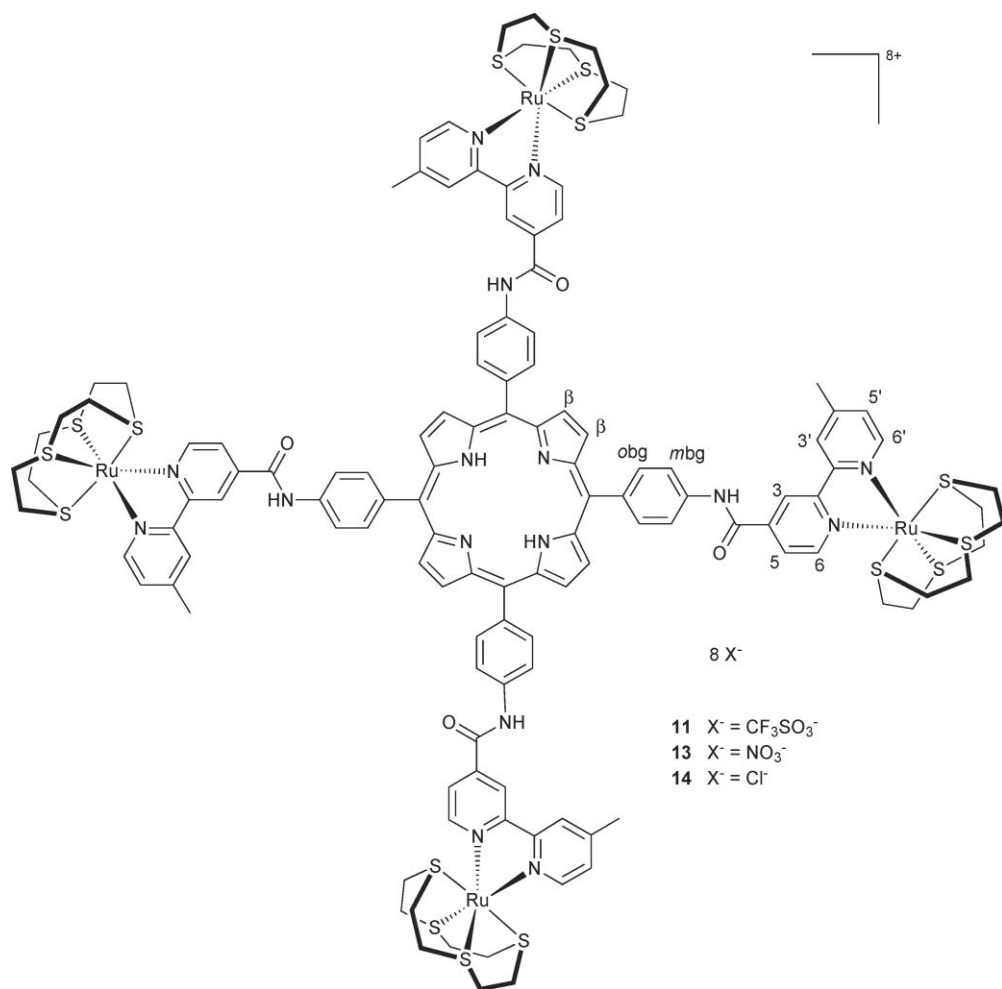


Fig. 12 Schematic drawing of conjugates 11, 13, and 14.

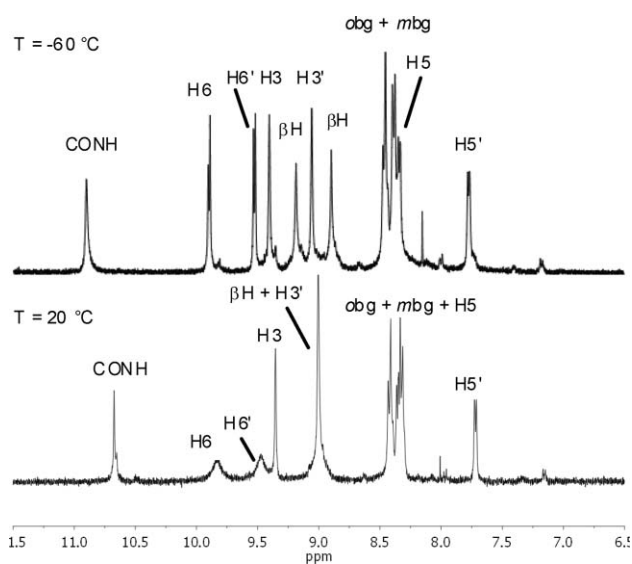


Fig. 13 Aromatic region in the ^1H NMR spectrum of $[\text{bpy}_4\text{-PP}\{\text{Ru}([\text{12}]\text{janeS4})_4\}[\text{CF}_3\text{SO}_3]_8$ (11) in acetone- d_6 at $20\text{ }^\circ\text{C}$ (bottom) and at $-60\text{ }^\circ\text{C}$ (top). See Fig. 12 for numbering scheme.

to the number of peripheral ruthenium compounds and to their relative charge. It is extremely difficult to predict if such conjugates might show some kind of interesting biological activity, perhaps through preferential interactions with specific biomolecules.

As anticipated above, we can however suggest two fields in which the positively charged porphyrin–Ru conjugates described in this work might deserve being investigated: as inhibitors of human telomerase and of K^+ channels.

Telomerase is a potential selective target for the design of new antitumour drugs, since it is an enzyme involved in the immortality of cancer cells (*i.e.* it is needed for tumour cell proliferation).^{54,55} One approach for inhibiting telomerase activity is to target the G-quadruplex DNA that is associated with the telomerase reaction cycle.^{56,57} The G-quadruplex is made by four guanine residues with a square-like geometry and an electron-rich π surface. Positively charged planar π -delocalized molecules, including metal compounds, have been demonstrated to be effective quadruplex binders.^{58,59} Cationic *meso*-tetrasubstituted porphyrins, by virtue of their intrinsic four-fold symmetry, are likely to provide an appropriate stereo-electronic match for G-quartets. Indeed, 5,10,15,20-tetrakis-(*N*-methyl)-4-pyridylporphyrin (TMPyP4) and its derivatives are a family of effective inhibitors of human telomerase in cell-free systems.^{60–62} Recent structural results suggest that

cationic porphyrins with relatively long and flexible side-arms might be better binders of G-quartets compared to TMPyP4 as they might allow stacking of the G-tetrad with the aromatic porphyrin core and minimize steric clashes with the G-tetrad edges.⁶² Appropriately designed inhibitors should bind more strongly to quadruplex DNA than to duplex DNA, so that relevant inhibition of telomerase activity can be achieved at subcytotoxic concentrations (*i.e.* concentrations that do not have general toxic effects on healthy cells). Indeed, Meunier and co-workers reported that a Mn(III) porphyrin with four flexible cationic arms at *meso* positions inhibits human telomerase at submicromolar concentration and, most importantly, binds G-quadruplex DNA four orders of magnitude more strongly than duplex DNA.⁶³

Finally, a number of cationic porphyrins with four-fold symmetry were found to bind with nanomolar affinity to K⁺ channels, and partially block their conductance, presumably by simultaneous interaction with all four channel subunits (most likely through salt bridges).⁶⁴

It would be therefore of interest to extend those investigations to poly-cationic tetra-ruthenated porphyrins such as those described in this work.

Conclusions and perspectives

In this work we have described different synthetic approaches to the preparation of porphyrin conjugates with Ru(III) and Ru(II) coordination compounds. We have varied the number and charge of the peripheral Ru fragments, and described conjugates whose total charge ranges from -4 to +8. The connection can occur through a single N(pyridyl)-Ru bond or through a chelating bpy unit. The Ru compounds can either contain one or more labile ligands (*functional compounds*) or be coordinatively saturated and substitutionally inert (*structural compounds*).

Meso-pyridylporphyrins (PyPs), beside being synthetically more affordable, allow to tune the geometry of the conjugates. We have shown that when 3'PyPs, instead of 4'PyPs, are used, the peripheral metal fragments typically lay both above and below the plane of the chromophore, thus giving access to diverse shapes and geometries.⁵⁰ The geometrical parameter might be relevant in particular when the porphyrins are conjugated to substitutionally inert metal fragments. In fact, the non-coordinative interactions between biomolecules and porphyrin conjugates with *structural* metal compounds might be affected significantly by the geometry of the porphyrin. For the time being we have exploited 4'PyPs exclusively, but the work might be easily extended also to the corresponding Ru conjugates with 3'PyPs.

In the series of porphyrins with peripheral bpy units at *meso* positions described in this work, bpy_n-PPs, the linker is relatively short and rigid. We are currently working to the development of novel four-fold symmetrical bpy₄-PPs in which the length and flexibility of the connectors between the bpyAc peripheral moieties and the *meso* C atoms are gradually increased. These novel porphyrins will then be conjugated to Ru compounds. An appropriate choice of the connector might also improve the solubility of the conjugates in aqueous solution.

Finally, even though we report here free-base porphyrin conjugates exclusively, it can be anticipated that insertion of metal ions such as Zn(II) and Cu(II) in the porphyrin core can be easily accomplished. Porphyrin metallation could be performed

either before or after conjugation, depending on the nature of the peripheral ruthenium fragments.

Acknowledgements

Financial support from Regione FVG, Fondazione CRTrieste, Fondo Trieste, COST D39, and Fondazione Beneficentia Stiftung is gratefully acknowledged. Fondazione CRTrieste is also gratefully acknowledged for the munificent donation of a Varian 500 NMR spectrometer to the Department of Chemical Sciences. A generous donation of hydrated ruthenium chloride from BASF Italia Srl is also gratefully acknowledged.

References

- 1 K. Szaciłowski, W. Macyk, A. Drzewiecka-Matuszek, M. Brindell and G. Stochel, *Chem. Rev.*, 2005, **105**, 2647; E. S. Nyman and P. H. Hynninen, *J. Photochem. Photobiol. B*, 2004, **73**, 1; H. Ali and J. E. van Lier, *Chem. Rev.*, 1999, **99**, 2379.
- 2 M. R. Detty, S. L. Gibson and S. J. Wagner, *J. Med. Chem.*, 2004, **47**, 3897.
- 3 M. C. DeRosa and R. J. Crutchley, *Coord. Chem. Rev.*, 2002, **233–234**, 351.
- 4 A. R. M. Chen-Collins, D. W. Dixon, A. N. Vzorov, L. G. Marzilli and R. W. Compans, *BMC Infectious Diseases*, 2003, **3**, 9; R. Song, M. Witvrouw, D. Schols, A. Robert, J. Balzarini, E. De Clercq, J. Bernadou and B. Meunier, *Antiviral Chem. Chemother.*, 1997, **8**, 85.
- 5 J. P. C. Tomè, M. G. P. M. S. Neves, A. C. Tomè, J. A. S. Cavaleiro, M. Soncin, M. Magaraggia, S. Ferro and G. Jori, *J. Med. Chem.*, 2004, **47**, 6649.
- 6 M. G. H. Vicente, *Curr. Med. Chem.: Anti-Cancer Agents*, 2001, **1**, 175; W. Tronconi, A. Colombo, M. Decesare, R. Marchesini, K. W. Woodburn, J. A. Reiss, D. R. Phillips and F. Zunino, *Cancer Lett.*, 1995, **88**, 41; K. W. Woodburn, G. C. A. Phillips Bellinger, M. Sadek, R. T. C. Brownlee and J. M. Reiss, *Bioorg. Med. Chem. Lett.*, 1992, **2**, 343.
- 7 C. Lottner, R. Knuechel, G. Bernhardt and H. Brunner, *Cancer Lett.*, 2004, **203**, 171; C. Lottner, K.-C. Bart, G. Bernhardt and H. Brunner, *J. Med. Chem.*, 2002, **45**, 2064; C. Lottner, K.-C. Bart, G. Bernhardt and H. Brunner, *J. Med. Chem.*, 2002, **45**, 2079; H. Brunner, K.-M. Schellerer and B. Treittinger, *Inorg. Chim. Acta*, 1997, **264**, 67; H. Brunner and H. Obermeier, *Angew. Chem., Int. Ed. Engl.*, 1994, **33**, 2214.
- 8 R. Song, Y.-S. Kim, C. O. Leed and Y. S. Sohn, *Tetrahedron Lett.*, 2003, **44**, 1537; R. Song, Y.-S. Kim and Y. S. Sohn, *J. Inorg. Biochem.*, 2002, **89**, 83.
- 9 L. Monsù-Scolaro, C. Donato, M. Castriciano, A. Romeo and R. Romeo, *Inorg. Chim. Acta*, 2000, **300–302**, 978.
- 10 M. J. Clarke, *Coord. Chem. Rev.*, 2003, **236**, 209; M. J. Clarke, F. Zhu and D. Frasca, *Chem. Rev.*, 1999, **99**, 2511.
- 11 I. Bratsos, S. Jedner, T. Gianferrara and E. Alessio, *Chimia*, 2007, **61**, 692; E. Alessio, G. Mestroni, A. Bergamo and G. Sava, *Met. Ions Biol. Syst.*, 2004, **42**, 323; E. Alessio, G. Mestroni, A. Bergamo and G. Sava, *Curr. Top. Med. Chem.*, 2004, **4**, 1525; M. Bacac, A. C. G. Hotze, K. von der Schilden, J. G. Haasnoot, S. Pacor, E. Alessio, G. Sava and J. Reedijk, *J. Inorg. Biochem.*, 2004, **98**, 402.
- 12 M. A. Jakupec, M. Galanski, V. B. Arion, C. G. Hartinger and B. K. Keppler, *Dalton Trans.*, 2008, 183; C. G. Hartinger, M. A. Jakupec, S. Zorbas-Seifried, M. Groessl, A. Egger, W. Berger, H. Zorbas, P. J. Dyson and B. K. Keppler, *Chem. Biodiversity*, 2008, **5**, 2140; C. G. Hartinger, S. Zorbas-Seifried, M. A. Jakupec, B. Kynast, H. Zorbas and B. K. Keppler, *J. Inorg. Biochem.*, 2006, **100**, 891; M. A. Jakupec and B. K. Keppler, *Curr. Top. Med. Chem.*, 2004, **4**, 1575.
- 13 S. J. Dougan and P. J. Sadler, *Chimia*, 2007, **61**, 704; Y. K. Yan, M. Melchart, A. Habtemariam and P. J. Sadler, *Chem. Commun.*, 2005, 4764; H. Chen, J. A. Parkinson, R. E. Morris and P. J. Sadler, *J. Am. Chem. Soc.*, 2003, **125**, 173.
- 14 P. J. Dyson, *Chimia*, 2007, **61**, 698; W. H. Ang and P. J. Dyson, *Eur. J. Inorg. Chem.*, 2006, 4003.
- 15 F. Schmitt, P. Govindaswamy, O. Zava, G. Süss-Fink, L. Juillierat-Jeanneret and B. Therrien, *JBIC, J. Biol. Inorg. Chem.*, 2009, **14**, 101;

- F. Schmitt, P. Govindaswamy, G. Süß-Fink, W. Han Ang, P. J. Dyson, L. Juillerat-Jeanneret and B. Therrien, *J. Med. Chem.*, 2008, **51**, 1811.
- 16 M. J. Rose and P. K. Mascharak, *Coord. Chem. Rev.*, 2008, **252**, 2093; M. J. Rose, N. L. Fry, R. Marlow, L. Hinck and P. K. Mascharak, *J. Am. Chem. Soc.*, 2008, **130**, 8834; M. J. Rose and P. K. Mascharak, *Chem. Commun.*, 2008, 3933.
- 17 S. Weckler, A. Mikhailovsky and P. C. Ford, *J. Am. Chem. Soc.*, 2004, **126**, 13566; C. L. Conrado, S. Weckler, C. Egler, D. Magde and P. C. Ford, *Inorg. Chem.*, 2004, **43**, 5543.
- 18 T. Gianferrara, B. Serli, E. Zangrando, E. Iengo and E. Alessio, *New J. Chem.*, 2005, **29**, 895.
- 19 T. Gianferrara, I. Bratsos, E. Alessio, *Dalton Trans.*, 2009, 10.1039/b905798f.
- 20 E. Iengo, F. Scandola and E. Alessio, *Struct. Bonding*, 2006, **121**, 105; F. Scandola, C. Chiorboli, A. Prodi, E. Iengo and E. Alessio, *Coord. Chem. Rev.*, 2006, **250**, 1471.
- 21 J. T. Hupp, *Struct. Bonding*, 2006, **121**, 145.
- 22 I. Beletskaya, V. S. Tyurin, A. Yu. Tsvadze, R. Guillard and C. Stern, *Chem. Rev.*, 2009, **109**, 1659.
- 23 J. Manono, P. A. Marzilli, F. R. Fronczek and L. G. Marzilli, *Inorg. Chem.*, 2009, **48**, 5626; P. L. Bernad, Jr., A. J. Guerin, R. A. Haycock, S. L. Heath, C. A. Hunter, C. Raposo, C. Rotger, L. D. Sarson and L. R. Sutton, *New J. Chem.*, 2008, **32**, 525; I.-W. Hwang, T. Kamada, T. K. Ahn, D. M. Ko, T. Nakamura, A. Tsuda, A. Osuka and D. Kim, *J. Am. Chem. Soc.*, 2004, **126**, 16187; B. Zimmer, V. Bulach, M. W. Hosseini and A. De Cian, *Eur. J. Inorg. Chem.*, 2002, 3079; N. Kyriatskas, K. D. Benkstein, C. L. Stern, K. E. Splan, R. C. Johnson, K. A. Walters, F. W. M. Vanhelsmont and J. T. Hupp, *Eur. J. Inorg. Chem.*, 2002, 2818.
- 24 F. C. Anson, C. Shi and B. Steiger, *Acc. Chem. Res.*, 1997, **30**, 437.
- 25 H. E. Toma and K. Araki, *Coord. Chem. Rev.*, 2000, **196**, 307.
- 26 E. Iengo, E. Zangrando and E. Alessio, *Acc. Chem. Res.*, 2006, **39**, 841.
- 27 K. Araki, C. A. Silva, H. E. Toma, L. H. Catalani, M. H. G. Medeiros and P. Di Mascio, *J. Inorg. Biochem.*, 2000, **78**, 269; J. L. Ravanat, J. Cadet, K. Araki, H. E. Toma, M. H. Medeiros and P. Di Mascio, *Photochem. Photobiol.*, 1998, **68**, 698; J. Onuki, A. V. Ribas, M. H. G. Medeiros, K. Araki, H. E. Toma, L. H. Catalani and P. Di Mascio, *Photochem. Photobiol.*, 1996, **63**, 272.
- 28 H. Kon, K. Tsuge, T. Imamura, Y. Sasaki, S. Ishizaka and N. Kitamura, *Inorg. Chem.*, 2006, **45**, 6875.
- 29 C. Metcalfe and J. A. Thomas, *Chem. Soc. Rev.*, 2003, **32**, 215; K. E. Erkkila, D. T. Odom and J. K. Barton, *Chem. Rev.*, 1999, **99**, 2777.
- 30 M. Pauly, I. Kayser, M. Schmitz, M. Dicato, A. Del Guerzo, I. Kolber, C. Moucheron and A. Kirsch-De Mesmaeker, *Chem. Commun.*, 2002, 1086; C. Moucheron, A. Kirsch-De Mesmaeker and S. Choua, *Inorg. Chem.*, 1997, **36**, 584; J. P. Lecomte, A. Kirsch-De Mesmaeker, M. M. Feeney and J. M. Kelly, *Inorg. Chem.*, 1995, **34**, 6481.
- 31 H.-J. Yu, H. Chao, L. Jiang, L.-Y. Li, S.-M. Huang and L.-N. Ji, *Inorg. Chem. Commun.*, 2008, **11**, 553; M. T. Mongelli, J. Heinecke, S. Mayfield, B. Okyere, B. S. J. Winkel and K. J. Brewer, *J. Inorg. Biochem.*, 2006, **100**, 1983; B. Elias and A. Kirsch-De Mesmaeker, *Coord. Chem. Rev.*, 2006, **250**, 1627.
- 32 K. Davia, D. King, Y. Hong and S. Swavey, *Inorg. Chem. Commun.*, 2008, **11**, 584.
- 33 J. Liu, J.-W. Huang, P. Zhao, B. Fu, H.-C. Yu and L.-N. Ji, *Transition Met. Chem.*, 2006, **31**, 1040; W.-J. Mei, J. Liu, H. Chao, L.-N. Ji, A.-X. Li and J.-Z. Liu, *Transition Met. Chem.*, 2003, **28**, 852.
- 34 M. Cunningham, A. McCrate, M. Nielsen and S. Swavey, *Eur. J. Inorg. Chem.*, 2009, 1521; S. Rani-Beeram, K. Meyer, A. McCrate, Y. Hong, M. Nielsen and S. Swavey, *Inorg. Chem.*, 2008, **47**, 11278; M. Narra, P. Elliott and S. Swavey, *Inorg. Chim. Acta*, 2006, **359**, 2256.
- 35 D. G. McCafferty, B. M. Bishop, C. G. Wall, S. G. Hughes, S. L. Mecklenberg, T. J. Meyer and B. W. Erickson, *Tetrahedron*, 1995, **51**, 1093.
- 36 E. Alessio, M. Bolle, B. Milani, G. Mestroni, P. Faleschini, S. Geremia and M. Calligaris, *Inorg. Chem.*, 1995, **34**, 4716.
- 37 E. Iengo, E. Zangrando, E. Baiutti, F. Munini and E. Alessio, *Eur. J. Inorg. Chem.*, 2005, 1019.
- 38 B. Serli, E. Zangrando, T. Gianferrara, C. Scolaro, P. J. Dyson, A. Bergamo and E. Alessio, *Eur. J. Inorg. Chem.*, 2005, 3423.
- 39 I. Bratsos, S. Jedner, A. Bergamo, G. Sava, T. Gianferrara, E. Zangrando and E. Alessio, *J. Inorg. Biochem.*, 2008, **102**, 1120.
- 40 T. M. Santos, B. J. Goodfellow, J. Madureira, J. Pedrosa de Jesus, V. Félix and M. G. B. Drew, *New J. Chem.*, 1999, **23**, 1015.
- 41 E. Zangrando, N. Kulisic, F. Ravalico, I. Bratsos, S. Jedner, M. Casanova and E. Alessio, *Inorg. Chim. Acta*, 2009, **362**, 820.
- 42 T. Gianferrara, D. Giust, I. Bratsos and E. Alessio, *Tetrahedron*, 2007, **63**, 5006.
- 43 R. Luguay, L. Jaquinod, F. R. Fronczek, M. G. H. Vicente and K. M. Smith, *Tetrahedron*, 2004, **60**, 2757.
- 44 A. Bettelheim, B. A. White, S. A. Raybuck and R. W. Murray, *Inorg. Chem.*, 1987, **26**, 1009.
- 45 Z. Otwinowski and W. Minor, Processing of X-ray Diffraction Data Collected in Oscillation Mode, *Methods Enzymol.*, 1997, **276**, 307.
- 46 G. M. Sheldrick, *SHELXL-97, Programs for Crystal Structure Analysis (Release 97-2)*, University of Göttingen, Germany, 1998.
- 47 L. J. Farrugia, *J. Appl. Crystallogr.*, 1999, **32**, 837.
- 48 E. Alessio, M. Macchi, S. L. Heath and L. G. Marzilli, *Inorg. Chem.*, 1997, **36**, 5614.
- 49 I. Bratsos, G. Birarda, S. Jedner, E. Zangrando and E. Alessio, *Dalton Trans.*, 2007, 4048.
- 50 M. Casanova, E. Zangrando, E. Iengo, E. Alessio, M. T. Indelli, F. Scandola and M. Orlandi, *Inorg. Chem.*, 2008, **47**, 10407.
- 51 A. Gabriellson, J. R. Lindsay Smith and R. N. Perutz, *Dalton Trans.*, 2008, 4259; A. Gabriellson, F. Hartl, H. Zhang, J. R. Lindsay Smith, M. Towrie and A. Vleck, Jr., *J. Am. Chem. Soc.*, 2006, **128**, 4253; R. N. Perutz, C. J. Aspley, J. R. Lindsay Smith and R. N. Perutz, *J. Chem. Soc., Dalton Trans.*, 1999, 2269; A. Gabriellson, F. Hartl, J. R. Lindsay Smith and R. N. Perutz, *Chem. Commun.*, 2002, 950.
- 52 X. Liu, J. Liu, J. Pan, R. Chen, Y. Na, W. Gao and L. Sun, *Tetrahedron*, 2006, **62**, 3674.
- 53 H. Adams, A. M. Amado, V. Felix, B. E. Mann, J. Antelo-Martinez, M. Newell, P. J. A. Ribeiro-Claro, S. E. Spey and J. Thomas, *Chem.-Eur. J.*, 2005, **11**, 2031.
- 54 P. Phatak and A. M. Burger, *Br. J. Pharmacol.*, 2007, **152**, 1003.
- 55 C. B. Harley, *Nat. Rev. Cancer*, 2008, **8**, 167.
- 56 E. M. Rezler, D. J. Bearss and L. H. Hurley, *Curr. Opin. Pharmacol.*, 2002, **2**, 415.
- 57 A. De Cian, L. Lacroix, C. Douarre, N. Temime-Smaali, C. Trentesaux, J. F. Riou and J.-L. Mergny, *Biochimie*, 2008, **90**, 131.
- 58 A. Arola-Arnal, J. Benet-Buchholz, S. Neide and R. Vilar, *Inorg. Chem.*, 2008, **47**, 11910.
- 59 R. Kiełtyka, P. Englebienne, J. Fakhoury, C. Autexier, N. Moitessier and H. F. Sleiman, *J. Am. Chem. Soc.*, 2008, **130**, 10040.
- 60 J. Seenisamy, S. Bashyam, V. Gokhale, H. Vankayalapati, D. Sun, A. Siddiqui-Jain, N. Streiner, K. Shin-ya, E. White, W. D. Wilson and L. H. Hurley, *J. Am. Chem. Soc.*, 2005, **127**, 2944; M.-Y. Kim, M. Gleason-Guzman, E. Izbicka, D. Nishioka and L. H. Hurley, *Cancer Res.*, 2003, **63**, 3247; H. Han, D. R. Langley, A. Rangan and L. H. Hurley, *J. Am. Chem. Soc.*, 2001, **123**, 8902; D. F. Shi, R. T. Wheelhouse, D. Sun and L. H. Hurley, *J. Med. Chem.*, 2001, **44**, 4509; F. X. Han, R. T. Wheelhouse and L. H. Hurley, *J. Am. Chem. Soc.*, 1999, **121**, 3561; R. T. Wheelhouse, D. Sun, H. Han, F. X. Han and L. H. Hurley, *J. Am. Chem. Soc.*, 1998, **120**, 3261.
- 61 P. Wang, L. Ren, H. He, F. Liang, X. Zhou and Z. Tan, *ChemBioChem*, 2006, **7**, 1155.
- 62 G. N. Parkinson, R. Ghosh and S. Neidle, *Biochemistry*, 2007, **46**, 2390.
- 63 I. M. Dixon, F. Lopez, A. M. Tejera, J. P. Esteve, M. A. Blasco, G. Pratiel and B. Meunier, *J. Am. Chem. Soc.*, 2007, **129**, 1502.
- 64 S. N. Gradl, J. P. Felix, E. Y. Isacoff, M. L. Garcia and D. Trauner, *J. Am. Chem. Soc.*, 2003, **125**, 12668.